EUROPEAN ORGANIZATION FOR NUCLEAR RESEARCH (CERN)

CERN-EP-2025-296
2026/07/22

CMS-EXO-24-020

Search for the pair production of long-lived supersymmetric partners of the tau lepton in proton-proton collisions at $\sqrt{s} = 13\,\text{TeV}$

The CMS Collaboration*

arXiv:2601.17576v2 [hep-ex] 21 Jul 2026

Abstract

Gauge-mediated supersymmetry-breaking models provide a strong motivation to search for a supersymmetric partner of the tau lepton (stau) with a macroscopic lifetime. Long-lived stau decays produce tau leptons that are displaced from the primary proton-proton interaction vertex, leading to an unconventional signature. This paper presents a search for the direct production of long-lived staus decaying within the CMS tracker volume in proton-proton collisions at $\sqrt{s} = 13\,\text{TeV}$, performed for the first time with an identification algorithm based on a graph neural network dedicated to displaced tau leptons. The data sample, corresponding to an integrated luminosity of $138\,\text{fb}^{-1}$, was recorded with the CMS experiment at the CERN LHC between 2016 and 2018. This search excludes, at 95% confidence level, stau masses, $m_{\tilde{\tau}}$, in the 126–260 (90–425) GeV range for a proper decay length of 50 mm in the maximally mixed (mass-degenerate) scenario, while for $m_{\tilde{\tau}} = 200\,\text{GeV}$, stau proper decay lengths are excluded in the range 21–94 (6–333) mm. These results improve the exclusion limits compared to previous searches, and extend the parameter space explored in the context of supersymmetry.

Published in the Journal of High Energy Physics as doi:10.1007/JHEP07(2026)102.

© 2026 CERN for the benefit of the CMS Collaboration. CC-BY-4.0 license

*See Appendix A for the list of collaboration members

1 Introduction

Supersymmetry (SUSY) [1–8] is an extension of the standard model (SM) of particle physics that offers potential solutions to several of its open questions, e.g., it can naturally account for the observed Higgs boson mass without resorting to fine-tuning of the bare mass [9–20]. In SUSY models, each SM particle is assigned a corresponding superpartner with the same quantum numbers, but differing in spin by half a unit. The contributions of SM particles and their superpartners to quantum corrections of the Higgs boson mass could partially cancel and thereby resolve the fine-tuning problem. In SUSY models with R-parity conservation [21], the lightest SUSY particle (LSP) is stable [22, 23] and could be a viable dark-matter candidate [24].

The superpartners of the electroweak gauge and Higgs bosons, referred to as bino, wino, and Higgsino, mix to form neutral and charged mass eigenstates, called neutralinos ($\widetilde{\chi}_{\mathrm{i}}^{0}$) and charginos ($\widetilde{\chi}_{\mathrm{i}}^{\pm}$). The SUSY partners of the leptons are called sleptons ($\widetilde{\ell}$), with stau ($\widetilde{\tau}$) referring to the tau lepton superpartner. For the third generation, the mass eigenstates ($\widetilde{\tau}_1$, $\widetilde{\tau}_2$) can have different masses (by definition, $\widetilde{\tau}_1$ is the lighter one) and are a mixture of the gauge eigenstates ($\widetilde{\tau}_{\mathrm{R}}$, $\widetilde{\tau}_{\mathrm{L}}$). This mixing can become large and depends on the Higgsino mass parameter, the ratio of the vacuum expectation values of the two Higgs fields ($\tan\beta$), and the third-generation A-parameter (A_τ) [25].

In gauge-mediated SUSY breaking [26–28] models, the gravitino ($\widetilde{\mathrm{G}}$) mass is proportional to the ratio of the SUSY-breaking scale F to the Planck energy scale. The $\widetilde{\mathrm{G}}$ is thus very light and is the LSP. In such models, the stau is a preferred candidate for the next-to-LSP, and $\widetilde{\tau} \rightarrow \tau\widetilde{\mathrm{G}}$ is the only available decay mode of the stau. The $\widetilde{\tau}-\tau-\widetilde{\mathrm{G}}$ coupling is suppressed by a factor of $1/F$, which leads to longer lifetimes for the stau. These scenarios can be investigated by searching for staus at proton colliders.

Searches for prompt $\widetilde{\tau}$ decays have been performed at the CERN LEP collider [29–32], excluding at 95% confidence level (CL) some scenarios with $\widetilde{\tau}$ masses, $m_{\widetilde{\tau}}$, up to about 90 GeV and neutralino masses up to about 80 GeV. The ATLAS and CMS Collaborations have searched for both promptly decaying and long-lived staus in proton-proton (pp) collisions at $\sqrt{s} = 13$ TeV at the CERN LHC [33–39]. These searches excluded promptly decaying $\widetilde{\tau}$ masses below 400 GeV for nearly massless neutralinos or gravitinos, assuming the production of mass-degenerate $\widetilde{\tau}_{\mathrm{L}}$ and $\widetilde{\tau}_{\mathrm{R}}$. The limits on $\widetilde{\tau}$ masses for the long-lived searches at $\sqrt{s} = 13$ TeV vary depending on the proper decay length ($c\tau_0$) of the stau, but are of the same order of magnitude as in the prompt scenarios. A recent search for displaced leptons by the ATLAS Collaboration [40] included data collected at $\sqrt{s} = 13.6$ TeV to exclude $\widetilde{\tau}$ masses up to 440 GeV for $c\tau_0 = 90$ mm. In a scenario with maximal mixing between $\widetilde{\tau}_{\mathrm{L}}$ and $\widetilde{\tau}_{\mathrm{R}}$, $m_{\widetilde{\tau}}$ values between 150 and 220 GeV have been excluded for $c\tau_0 = 0.1$ mm at CMS with pp collisions at $\sqrt{s} = 13$ TeV [36]. Both ATLAS and CMS have also performed searches at $\sqrt{s} = 8$ TeV [41–43].

The existing searches for long-lived staus that decay sufficiently within the tracker volume can be broadly divided into two categories. The first category consists of generic searches for long-lived charged particles with final states containing electrons or muons from leptonic τ decays, which provide interpretations for long-lived staus. These searches profit from the clean signatures of the leptons. The second category consists of searches with hadronically decaying tau leptons (τ_{h}), which target the dominant τ decay mode, and are based on reconstruction and identification algorithms optimized for τ_{h} candidates produced from prompt decays of particles [44, 45]. Such algorithms lose efficiency rapidly as the transverse distance of the decay vertex from the beam axis increases, falling by ≈95% at around 10 mm [46], thereby reducing the sensitivity of a search for staus with higher $c\tau_0$.

This paper focuses on the search for long-lived staus decaying into a τ and a nearly massless (1 GeV) $\widetilde{\mathrm{G}}$, as shown in Fig. 1, within the framework of simplified models with masses between 90 and 600 GeV and $c\tau_0$ between 1 and 1000 mm [47, 48]. Since tau leptons decay to hadrons more often than to electrons and muons [25], this search targets the mode where both the tau leptons decay hadronically. In order to overcome aforementioned limitations of existing τ_{h} identification algorithms, a dedicated algorithm based on the PARTICLENET [49] graph convolutional neural network has been developed to identify τ_{h} produced far from the pp collision vertex, i.e., displaced ($\tau_{\mathrm{h}}^{\mathrm{dis}}$). This is referred to as the DISTAU identification algorithm [46].

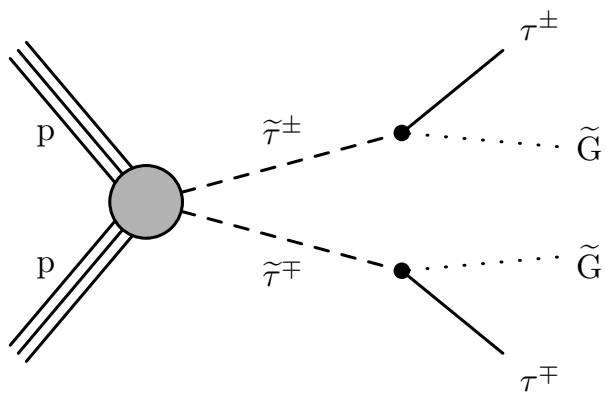

Figure 1: Diagram of stau pair production in pp collisions at the LHC, and the decay that leads to a final state with pairs of tau leptons accompanied by gravitinos.

This paper is organized as follows. The CMS detector is introduced in Section 2, and the event simulation is detailed in Section 3. Section 4 contains the event reconstruction. The event selection and background estimation are described in Sections 5 and 6, respectively. The systematic uncertainties are discussed in Section 7, and the results are presented in Section 8. A summary is given in Section 9. Tabulated results are provided in the HEPData record for this analysis [50].

2 The CMS detector

The central feature of the CMS apparatus is a superconducting solenoid of 6 m internal diameter that provides a magnetic field of 3.8 T. Within the solenoid volume are a silicon pixel and strip tracker, a lead tungstate crystal electromagnetic calorimeter (ECAL), and a brass and scintillator hadron calorimeter (HCAL), each composed of a barrel and two endcap sections. Forward calorimeters extend the coverage in pseudorapidity (η) provided by the barrel and endcap detectors. Muons are detected in gas-ionization chambers embedded in the steel flux-return yoke outside the solenoid. A more detailed description of the CMS detector, together with a definition of the coordinate system used and the relevant kinematic variables, is provided in Refs. [51, 52].

Events of interest are selected using a two-tiered trigger system. The first level, composed of custom hardware processors, uses information from the calorimeters and muon detectors to select events at a rate of around 100 kHz within a fixed latency of 4 μs [53]. The second level, known as the high-level trigger, consists of a farm of processors running a version of the full event reconstruction software optimized for fast processing, and it reduces the event rate to a few kHz before data storage [54, 55].

3 Event simulation

Several Monte Carlo (MC) event generators are used to simulate events for the signal and background processes. The signal process shown in Fig. 1 is simulated based on simplified SUSY models. The simulation is performed at leading order (LO) using the MADGRAPH5_aMC@NLO v2.4.2 event generator [56]. The NNPDF3.0 parton distribution function (PDF) set [57] is used for simulated samples corresponding to the 2016 data-taking period, whereas NNPDF3.1 [58] is used for 2017 and 2018. The signal cross sections are evaluated for a set of discrete $m_{\widetilde{\tau}}$ values between 90 and 600 GeV at next-to-LO (NLO) in perturbative quantum-chromodynamics calculations (pQCD), using next-to-leading logarithmic (NLL) soft-gluon threshold resummation, as provided by RESUMMINO [59–64]. The cross sections for $m_{\widetilde{\tau}}$ between the values that are reported in the aforementioned references are interpolated using the HEPI-FAST tool [65]. For each $m_{\widetilde{\tau}}$ hypothesis, signal samples have been simulated with stau $c\tau_0$ values ranging from 1 to 600 mm. Two different cases have been considered for the stau pair production in this study. The first is the production of $\widetilde{\tau}_1\overline{\widetilde{\tau}}_1$ in a "maximally mixed scenario", where the mixing angle between $\widetilde{\tau}_L$ and $\widetilde{\tau}_R$ is $\pi/4$, and $\widetilde{\tau}_2$ is considered to be too massive to be produced at the LHC. The second scenario is the production of both $\widetilde{\tau}_L\overline{\widetilde{\tau}}_L$ and $\widetilde{\tau}_R\overline{\widetilde{\tau}}_R$ with no mixing between the gauge eigenstates. Since in this case the gauge eigenstates are the same as the mass eigenstates, which are considered to be degenerate in mass, this is referred to as the "mass-degenerate scenario" in this paper. The mass-degenerate scenario leads to a cross section between three and five times higher than the maximally mixed scenario for each $m_{\widetilde{\tau}}$ considered. This is because in the s-channel production of stau pairs via Z/γ^*, $\widetilde{\tau}_L$ has a stronger coupling to the Z boson than $\widetilde{\tau}_R$, but both couple equally to the photon.

In this search, the contribution from background processes is estimated using control samples in data, as detailed in Section 6. Simulated events are used to validate the background estimation procedure based on data, and to train and calibrate the identification algorithm discussed in Section 4.2. Simulated samples of top quark-antiquark pair production ($t\bar{t}$), single top quark production, and $t\bar{t}V$ (V = W or Z) events are generated with the POWHEG 2.0 generator [66–70] at NLO in pQCD. Diboson (VV and VH) events are simulated at NLO with the MADGRAPH5_aMC@NLO 2.6.5 generator. The MADGRAPH (v2.2.2 for 2016, v2.4.2 for 2017 and 2018) [56] event generator is used at LO for modeling the Drell–Yan+jets (DY+jets) and W+jets processes, as well as for SM events comprised uniquely of jets produced through the strong interaction, referred to as multijet events.

The kinematic variables are generated including representative distributions of additional pp interactions per bunch crossing, referred to as pileup. These samples are produced separately for each year of data taking to account for different pileup and detector conditions in the three years. Additionally, the simulated samples for each year are reweighted such that their pileup profiles match the one measured in the data of the corresponding year.

The CMS detector response for all processes is modeled using GEANT4 [71], and simulated events are then reconstructed in the same way as collision data. For all simulated events, the description of parton showering and hadronization, as well as the hadronic decays of tau leptons, is performed with PYTHIA v8.212 [72] with the CP5 underlying event tune [73].

Small discrepancies observed between simulation and data are removed by using several correction factors, as discussed in Section 7.

4 Event reconstruction

4.1 Standard object reconstruction

A particle-flow (PF) algorithm [74] reconstructs each individual particle in an event, with an optimized combination of information from various components of the CMS detector. The energies of electrons and photons are measured in the ECAL. The momentum of electrons is determined by a combined measurement of the track momentum in the tracker, the energy of the matching ECAL supercluster, and the energy of all bremsstrahlung photons consistent with originating from the track. The momentum of muons is obtained from the bending of the corresponding tracks in the tracker and the muon spectrometer, which comprises three technologies: drift tubes, cathode strip chambers, and resistive plate chambers. The energy of charged hadrons, which is corrected for the response function of the calorimeters to hadronic showers, is determined from a combination of the momentum measured in the tracker and the energy of the matching ECAL and HCAL clusters. Finally, the energy of neutral hadrons is obtained from the corrected energies in the corresponding ECAL and HCAL clusters.

Collision vertices are reconstructed by fitting tracks in an event and are required to be within 24 cm of the center of the detector in the z direction (along the beam) and to have a transverse displacement from the beam line of less than 2 cm. The primary vertex is taken to be the vertex corresponding to the hardest scattering in the event, evaluated using tracking information alone, as described in Section 9.4.1 of Ref. [75]. Reconstruction of jets is performed by clustering PF objects using the anti-k_{T} algorithm [76, 77] with a distance parameter of $R = 0.4$. The jet momentum is determined as the vector sum of all particle momenta in the jet and is typically within 5–10% of the true momentum over the entire p_{T} spectrum within the detector acceptance. Pileup interactions contribute to spurious tracks and calorimetric energy deposits, increasing the apparent jet momentum. To mitigate this effect, tracks identified as originating from pileup vertices are discarded, and an offset is applied to correct for the remaining contributions [78]. Jets are calibrated using information from both simulation and data [78]. Additional selection criteria are applied to remove jets that are potentially dominated by instrumental effects or reconstruction failures [79]. Only jets with $p_{\mathrm{T}} > 30\,\mathrm{GeV}$, $|\eta| < 2.1$, and containing at least one charged PF object with $p_{\mathrm{T}} > 1\,\mathrm{GeV}$ are considered in this analysis. The absolute transverse impact parameter ($|d_{xy}|$) of a jet and its impact parameter significance ($\hat{d}_{xy}$)—the ratio between $|d_{xy}|$ and its uncertainty—are defined as the $|d_{xy}|$ and $\hat{d}_{xy}$ of its charged constituent with the highest p_{T}. For nonisolated particles with $1 < p_{\mathrm{T}} < 10\,\mathrm{GeV}$ and $|\eta| < 3.0$, the track resolutions are typically 1.5% in p_{T} and 20–75 μm in d_{xy} [80]. Isolated particles with p_{T} = 100 GeV and $|\eta| < 1.4$ have track resolutions of 2.8% in p_{T} and 10 μm in d_{xy} [81]. Choosing the charged constituent with the highest p_{T} in jets originating from the fragmentation of partons may not be robust against infrared and collinear emissions in the parton shower simulation. However, this is expected to have a negligible impact on the analysis as the contribution of such jets to the background is estimated entirely using data, as detailed in Section 6.

Jets originating from the fragmentation of b quarks are identified as b-tagged jets [82] using the DEEPJET algorithm [83, 84]. The algorithm employs properties of reconstructed secondary vertices and charged and neutral particle constituents of the jet as inputs to a convolutional deep neural network. The "medium" selection or working point (WP) of this algorithm corresponds to a signal efficiency of about 80%, with a misidentification probability of about 1% for light-flavored jets (i.e., originating from gluons or up, down, and strange quarks) and about 11% for jets originating from charm quarks. Jets passing this WP are henceforth referred to as b-tagged jets.

Electrons are identified using the "loose" WP of a boosted decision tree algorithm [85, 86] that uses inputs based on the spatial distribution of the shower, track-to-cluster-matching criteria, consistency between the cluster energy and the track momentum, and isolation. Electrons satisfying the loose WP and with $p_T > 20\,\text{GeV}$ and $|\eta| < 2.4$ are referred to as veto-electrons in what follows.

Muon reconstruction uses a global fit combining information from the tracker and muon spectrometers [87]. Muon candidates are required to pass either the "loose" or the "tight" WP of an identification algorithm using criteria such as the quality of the global fit and the geometrical matching between the tracks in the tracker and the muon spectrometers. Isolation criteria are imposed on the muon candidates to reject those originating from hadronic decays. The isolation variable used for this purpose is defined as the scalar p_T sum of reconstructed charged and neutral particles within a cone of radius $\Delta R = \sqrt{(\Delta\eta)^2 + (\Delta\phi)^2} = 0.4$, where ϕ is the azimuthal angle in radians, around the muon candidate track, which is excluded from the sum, divided by the p_T of the lepton candidate. Charged particles not originating from the primary vertex are excluded from this sum, and a correction is applied to account for the neutral components originating from pileup, as described in Ref. [88]. Muons satisfying the tight (loose) WP and with relative isolation less than 15 (25)%, $p_T > 20$ (28) GeV, and $|\eta| < 2.4$, are referred to as veto-muons (id-muons) in what follows.

Hadronic tau lepton candidates are reconstructed from one charged hadron and up to two neutral pions, or three charged hadrons and up to one neutral pion, consistent with originating from the decay of a tau lepton, using the hadrons-plus-strips algorithm [44]. To distinguish between jets originating from quarks or gluons and genuine hadronic tau lepton decays, the discriminant of the DEEPTAU [45] deep neural network algorithm is used. The τ_h candidates are required to have $p_T > 30\,\text{GeV}$, $|\eta| < 2.4$, and are selected with the "medium" WP of the above discriminant, which has an efficiency of ≈70% and a misidentification probability of ≈1%. In addition, the τ_h candidates are required to satisfy the "very loose" ("medium") WP of the DEEPTAU discriminant against electrons (muons), which has an efficiency of ≈98 (99.8)% and a misidentification probability of ≈1.5 (0.04)%. These τ_h candidates are used to identify a region enriched in $Z \to \tau\tau$ events, where the calibration factors for the DISTAU identification efficiency are measured, as described in Section 4.2.

The missing transverse momentum vector, $\vec{p}_T^{\,miss}$, is computed as the negative vector $\vec{p}_T$ sum of all the PF objects in an event and its magnitude is denoted as p_T^{miss} [89]. The $\vec{p}_T^{\,miss}$ is modified to account for the energy calibration of all the PF candidates in an event, clustered into jets or not.

4.2 Displaced τ_h candidates

The DISTAU [46] graph neural network algorithm is trained to distinguish between signal jets originating from displaced τ_h candidates (τ_h^{dis}) and those from the fragmentation of light-flavored, charm, and bottom quarks, and gluons (background jets). The signal jets used for the training are selected from three different signal samples corresponding to $c\tau_0$ values of 1, 100, and 1000 mm. These samples are orthogonal to the ones used for obtaining the signal yields in Section 8. To use well-reconstructed signal jets for the training, the longitudinal (transverse) position of the stau decay vertex is required to be within 1000 mm (500 mm) of the interaction point, which is approximately the longitudinal (radial) extent of the inner tracker detector. No lower threshold is imposed on the signal jet displacement. Hence, the network is allowed to learn from signal jets with a wide range of displacements, arising from staus that decay within the inner tracker volume. The background jets are taken from multijet events, and

jets with different flavors are treated together as a single background category, as separating them by flavor did not provide any significant improvement in discrimination. Jets from τ_h candidates produced from prompt decays of particles are not treated as a separate background category as there is no distinctive difference in properties between them and signal jets with very small displacements. Moreover, the contribution from prompt τ_h produced in SM processes being misidentified as τ_h^{dis} candidates is sufficiently suppressed by the selection on jet d_{xy}, as discussed in Sections 5 and 6.

The algorithm, based on the PARTICLENET [49] architecture, represents the particles in a jet as a "point cloud" and performs dynamic graph convolution operations [90] on the properties of each jet constituent and its nearest neighbors. The features provided as input to the network are the same as those used in the DEEPTAU algorithm [45]. The DISTAU algorithm is optimized to identify τ_h^{dis} produced within the tracker volume of the CMS detector. The algorithm exploits features relevant for both hadronic τ decays (such as the number of charged hadrons and their isolation properties), as well as displaced τ decays (such as the impact parameters of the charged constituent tracks). Impact parameters are also used by the DEEPTAU algorithm as input features, but they play a more significant role in the discriminating power of the DISTAU algorithm. Displacements of less than 10 mm result in reduced discrimination between τ_h^{dis} candidates and background jets, while for displacements above around 500 mm, the τ_h^{dis} candidate cannot produce enough hits in the tracker to be distinguished from the track of the $\widetilde{\tau}$ that produced it, leading to a lower identification efficiency.

The distributions of DISTAU scores for signal and background jets are presented in Fig. 2. The "loose", "medium", and "tight" WPs of the DISTAU algorithm are denoted as WPL, WPM, and WPT, with signal efficiencies of about >99, 98, and 80%, respectively, measured in simulated events for a signal hypothesis of $m_{\widetilde{\tau}} = 200\,\text{GeV}$ and $c\tau_0 = 100\,\text{mm}$. Their respective misidentification probabilities, evaluated in simulated $t\bar{t}$ events, are approximately 7, 1, and 0.06%. The efficiencies (misidentification probabilities) quoted here are inclusive, i.e., measured with respect to all signal (background) jets in the simulated sample. The lower thresholds on the tagger score corresponding to the three WPs are 0.05, 0.7, and 0.99, respectively. To be chosen as a τ_h^{dis} candidate, a jet selected with the criteria mentioned in Section 4.1 is also required to satisfy $|d_{xy}| > 2\,\text{mm}$, $\hat{d}_{xy} > 5$, and pass the WPL selection. The requirement on $\hat{d}_{xy}$ ensures that the d_{xy} of the selected τ_h^{dis} candidates is well measured.

The efficiency of the DISTAU identification algorithm for the simulated signal is corrected to match the efficiency measured in data, using a control region (CR) enriched in DY($Z/\gamma^* \to \tau\tau$)+jets events, where one of the tau leptons decays to a muon and the other decays hadronically. This is referred to as the $\mu\tau_h$ CR. As there are no truly signal-like τ_h^{dis} candidates in SM processes, the τ_h in the event serves as a proxy to evaluate the identification efficiency. Following a strategy similar to that in Ref. [91], events are selected online with a single-muon trigger, and required to have exactly one id-muon and one τ_h candidate with opposite electric charges, angular separation $\Delta R(\mu, \tau_h) > 0.5$, invariant mass of the $\mu\tau_h$ system between 60 and 80 GeV, transverse mass $m_T(\mu, \vec{p}_T^{miss}) < 60\,\text{GeV}$, and $D_\zeta(\mu, \tau_h, \vec{p}_T^{miss}) > -25\,\text{GeV}$, with $D_\zeta(\mu, \tau_h, \vec{p}_T^{miss})$ defined as [91, 92]

$$D_\zeta(\mu, \tau_h, \vec{p}_T^{miss}) = \vec{p}_T^{miss} \cdot \hat{\zeta} - 0.85[\vec{p}_T(\mu) + \vec{p}_T(\tau_h)] \cdot \hat{\zeta}, \tag{1}$$

where $\hat{\zeta}$ is the unitary vector oriented along the bisector of the muon and the τ_h candidate transverse momenta, $\vec{p}_T(\mu)$ and $\vec{p}_T(\tau_h)$, respectively. The transverse mass for two objects la-

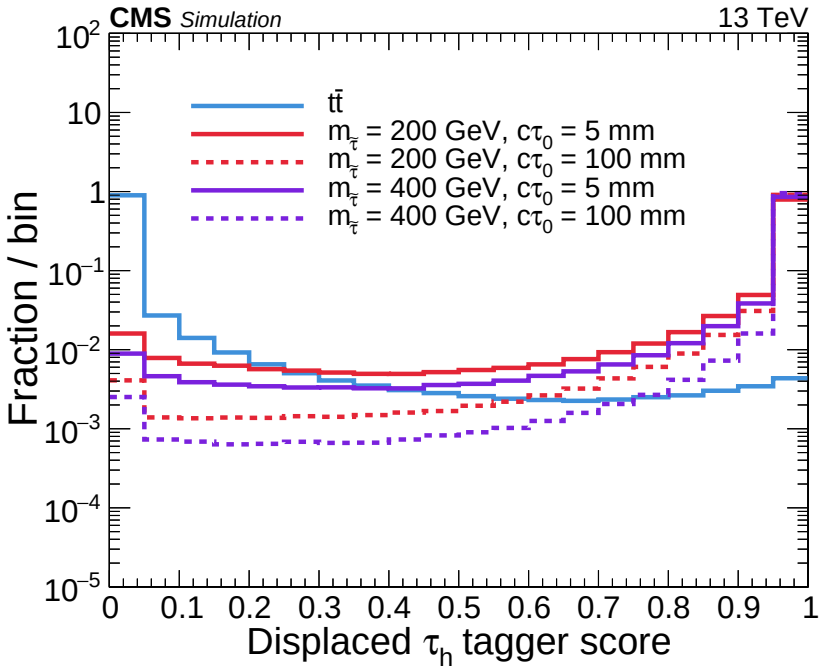

Figure 2: Distributions of DISTAU score for signal and background jets. The background jets are taken from simulated $t\bar{t}$ events where both top quarks decay hadronically, while signal jets are sampled from four representative ($m_{\tilde{\tau}}$ [GeV], $c\tau_0$ [mm]) hypotheses: (200, 5), (200, 100), (400, 5), and (400, 100). Each distribution is normalized such that its integral is unity.

beled "a" and "b" is defined as

$$m_T^2(a,b) = m_a^2 + m_b^2 + 2(E_T^a E_T^b - \vec{p}_T^{\,a} \cdot \vec{p}_T^{\,b}). \tag{2}$$

Here the masses (transverse momenta) of the particles are denoted by m_a and m_b ($\vec{p}_T^{\,a}$ and $\vec{p}_T^{\,b}$), respectively, and $E_T^2 = m^2 + p_T^2$. The $m_T(\mu, \vec{p}_T^{\,miss})$ formulation is then obtained by replacing the generic particles with a muon and a massless particle of transverse momentum $\vec{p}_T^{\,miss}$.

Correction factors are estimated using the "tag-and-probe" technique described in Refs. [44, 45, 93]. The muon serves as the "tag" in this procedure, while the τ_h^{dis} candidate nearest to the τ_h and satisfying $\Delta R(\tau_h, \tau_h^{dis}) < 0.4$ is treated as the "probe". The distribution of the DISTAU score for the probes in the $\mu\tau_h$ CR is shown in Fig. 3. To measure the simulation-to-data correction for a given WP, a maximum likelihood fit is performed on the invariant mass distribution of the $\mu\tau_h$ system, which offers a bounded (60–80 GeV, as stated above) distribution that includes probes of any momenta, provided they satisfy the requirements on jet p_T and $|\eta|$ discussed in Section 4.1. The fit is performed simultaneously for events in two regions: one in which the probe passes the chosen WP and one in which it fails. The correction to the DISTAU efficiency is then treated as an anticorrelated parameter across the two regions in the fit, in which the efficiency of the selected WP in simulation is corrected to match the one in data. This procedure yields a correction factor that can be applied to simulation for each τ_h^{dis} candidate (satisfying the chosen WP) in an event. The correction factor per τ_h^{dis} candidate for WPT is evaluated from the fit to be within 10% of unity for all years with an uncertainty of 0.15. The leading contribution to this uncertainty arises from the statistical uncertainty in the number of events that pass the WPT selection. The behavior of the correction factors with increasing probe jet d_{xy} has also been studied, and no significant dependence is observed. In Fig. 3, the small departures from unity in the ratio between data and predicted SM processes (≈10–15% in most bins) do not affect the measurement of the correction factors to any appreciable degree, as the fit is intended

to measure the difference in the efficiency of the WPT selection between data and simulation, and not the overall normalization difference.

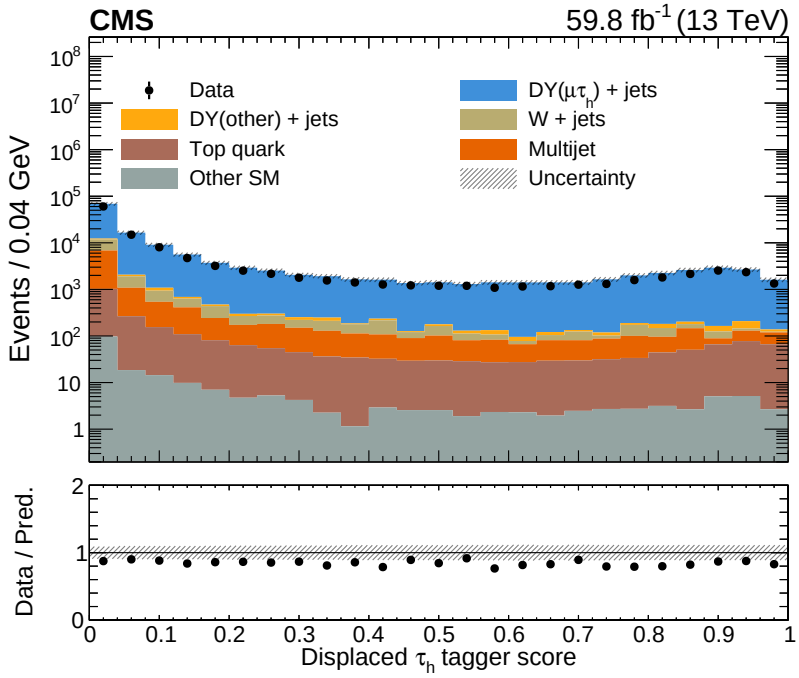

Figure 3: Distributions of DisTau score for τ_h^{dis} probes in the $\mu\tau_h$ CR described in Section 4.2, for data and predicted SM processes, corresponding to the 2018 data-taking period. Here DY($\mu\tau_h$) represents events from the $Z/\gamma^* \to \tau\tau$ process, where one of the tau leptons decays to a muon and the other decays hadronically. Events from other decay modes of Z/γ^* are denoted as DY(other). Processes denoted as "Top quark" comprise $t\bar{t}$, single top, and $t\bar{t}V$, and other SM processes include events from diboson production. Uncertainties in the simulation are shown as a grey band and include only the statistical uncertainty in the number of simulated events. Simulation is not fully calibrated to describe data, as the distribution is shown to illustrate the general behavior of the classifier and is not directly used for the measurement of simulation-to-data correction factors. The bars representing the statistical uncertainty in the data are not visible as they are smaller than the marker size. The results for the 2016 and 2017 data-taking periods are similar in behavior.

5 Event selection

In order to reject the vast majority of events that are easily identifiable as incompatible with the signal topology, we define a baseline region (BR) containing events in both the signal-enriched search region (SR) and the sideband regions that are used for estimating the background contribution in the SR.

Since the signal is expected to have high missing momentum from gravitinos that escape without interacting with the detector, events in the BR are selected with high-level triggers requiring a large transverse momentum imbalance: $p_T^{miss} > 100$ GeV in 2016 and $p_T^{miss} > 120$ GeV in 2017 and 2018. The efficiency of the p_T^{miss} triggers increases from about 70% at 120 GeV to a plateau of almost unity at 250 GeV. Offline, events are required to have $p_T^{miss} > 120$ GeV and exactly two τ_h^{dis} candidates. Since the offline requirement on p_T^{miss} is in the turn-on region of the trigger efficiency, the uncertainty in the trigger efficiency is treated differently for events with p_T^{miss}

below and above 250 GeV, as described in Section 7. Events are rejected if they have any veto-electron, veto-muon, or b-tagged jet. The leading (higher-p_T) and subleading (lower-p_T) τ_h^{dis} candidate jets in an event are referred to as j1 and j2, respectively. The background contribution from jets produced in noncollision processes, such as beam halo interactions, is greatly mitigated by requiring events to satisfy the beam halo filters [89]. Since beam halo jets usually populate the plane defined by the beam axis and $\phi = 0$ or π, their contribution is further reduced by requiring events to satisfy $\Delta\phi(\text{j1},\text{j2}) > 0.5$. In order to mitigate the impact of increased noise in the ECAL endcaps observed during the 2017 data-taking period, events with $H_T^{\text{soft, fwd}} > 50\,\text{GeV}$ are vetoed. Here $H_T^{\text{soft, fwd}}$ is defined as the scalar sum of the p_T of all soft (uncorrected $p_T < 50\,\text{GeV}$) jets in the forward region ($2.65 < |\eta| < 3.139$). Since jets in signal processes are typically harder and in the central region, this selection has a negligible effect on signal events, while suppressing background events. The requirement on $H_T^{\text{soft, fwd}}$ thus helps to improve sensitivity to the signal, and is applied to all data-taking periods.

A separate CR enriched in W+jets events (WCR) is selected using single-muon triggers. Offline, events are required to satisfy the aforementioned beam halo filters, have exactly one id-muon, no additional veto-muons or veto-electrons, $p_T^{\text{miss}} > 50\,\text{GeV}$, $60 < m_T(\mu, \vec{p}_T^{\text{miss}}) < 120\,\text{GeV}$, and exactly two τ_h^{dis} candidates satisfying the same requirement on $\Delta\phi(\text{j1},\text{j2})$ as in the BR. The region thus defined is about 85% pure in W+jets events.

Single-muon triggers are also used to identify another separate CR enriched in DY+jets (DYCR). Offline, events are required to satisfy the aforementioned beam halo filters, have exactly two id-muons with opposite charges, no additional veto-muons or veto-electrons, dimuon invariant mass between 70 and 120 GeV, and the same requirement on the τ_h^{dis} candidates as the WCR. This region is found to be approximately 96% pure in DY+jets events.

The contamination from signal processes in WCR and DYCR is found to be negligible (<1%) using simulation. Events satisfying the BR, WCR, and DYCR selections are categorized into the T0, T1, and T2 regions based on whether zero, one, or two jets, respectively, passed the DisTau WPT, as illustrated in Table 1. For example, BRT0 includes events in the BR satisfying the T0 selection. We use BRT2 as the SR, whereas BRT0, BRT1, WCR, and DYCR are CRs used for background estimation and validation, as described in Section 6. All the regions discussed here are mutually orthogonal.

Table 1: Signal and control region definitions. The observed number of events in each region is shown in parentheses.

Tag criteria	T0	T1	T2
Description	Exactly two τ_h^{dis} candidates of which none pass WPT	Exactly two τ_h^{dis} candidates of which only one passes WPT	Exactly two τ_h^{dis} candidates of which both pass WPT
Baseline selections	BRT0 (6287)	BRT1 (1384)	BRT2 ≡ SR (81)
W+jets CR selections	WCRT0 (5517)	WCRT1 (1094)	WCRT2 (86)
DY+jets CR selections	DYCRT0 (1156)	DYCRT1 (218)	DYCRT2 (18)

The dominant sources of p_T^{miss} in the signal events would be the weakly interacting gravitinos, whose kinematic properties are correlated with those of the visible objects, namely, the τ_h candidates. In contrast, p_T^{miss} in the SM background processes primarily originates from neutrinos. This difference can be exploited by first constructing the transverse mass $m_T(\text{vis}, \text{inv})$, defined in Eq. 2, with the visible ("vis") and the invisible ("inv") particles. The distribution of $m_T(\text{vis}, \text{inv})$ presents a maximum at the mass of the parent of the visible and the invisible particles when there is only one source of missing momentum in the system. To account for pair-produced particles where both have visible and invisible decay products, the "stransverse

mass (m_{T2})" [94, 95] is defined as:

$$m_{T2}^2(\text{vis1}, \text{vis2}, \vec{p}_T^{\text{miss}}) = \min_{\vec{p}_T^{\text{inv1}} + \vec{p}_T^{\text{inv2}} = \vec{p}_T^{\text{miss}}} [\max\{m_T^2(\text{vis1}, \text{inv1}), m_T^2(\text{vis2}, \text{inv2})\}]. \quad (3)$$

Since the momenta of the individual invisible particles in Eq. (3) are unknown, $\vec{p}_T^{\text{miss}}$ is divided into two components ($\vec{p}_T^{\text{inv1}}$ and $\vec{p}_T^{\text{inv2}}$) in such a way that the value of m_{T2} is minimized. If m_{T2} is computed using the two τ_h^{dis} candidates as the visible objects, "vis1" and "vis2", then its upper limit in the signal will be the stau mass. This is different from the SM background processes. For example, in $t\bar{t} \to b\bar{b}W^+W^-$ events, where both the W bosons decay to a lepton (visible) and a neutrino (invisible), the upper limit is at the W boson mass. In searches where the masses of the invisible particles are unknown, the calculation of m_{T2} requires an assumption on their masses [96]. In this analysis, we consider the gravitino to be massless when calculating m_{T2}.

In addition to p_T^{miss} and m_{T2}, the p_T of the subleading τ_h^{dis} candidate ($p_{T,\,j2}$) is found to be useful to discriminate between signal and background. Distributions of these three variables for events within the SR are presented in Fig. 4. The background distributions have been estimated using the procedure described in Section 6. Signal events with different $m_{\tilde{\tau}}$ populate different regions of the parameter space. For example, regions with low (high) p_T^{miss}, m_{T2}, and $p_{T,\,j2}$ are sensitive to signals with low (high) $m_{\tilde{\tau}}$. In order to have high sensitivity over a wide range of $m_{\tilde{\tau}}$, selected events are categorized into eight bins in the measured p_T^{miss}, m_{T2}, and $p_{T,\,j2}$, as shown in Table 2.

Table 2: The $p_{T,\,j2}$, p_T^{miss}, and m_{T2} requirements for each of the eight analysis bins.

Bin no.	$p_{T,\,j2}$ [GeV]	p_T^{miss} [GeV]	m_{T2} [GeV]
1	30–50	120–250	<100
2	30–50	120–250	>100
3	30–50	>250	—
4	50–100	120–250	<100
5	50–100	120–250	>100
6	50–100	>250	—
7	>100	—	<100
8	>100	—	>100

6 Background estimation

The dominant background in this search arises from light quark and gluon jets that are misidentified as τ_h^{dis} candidates. Such jets can be produced in SM processes from pp collisions, or in noncollision processes, such as beam halo interactions. The latter contribution is greatly mitigated with the selections discussed in Section 5. Jets arising from beam halo are mostly trackless and preferably populate the forward (high $|\eta|$) regions. Any residual contamination from beam halo is expected to be negligible as DisTau relies heavily on the properties of charged PF candidates in jets, and jets are required to have at least one charged PF candidate (i.e. a track) and be reconstructed within $|\eta| < 2.1$, as discussed in Section 4.1. The contribution to the background yield from electrons, muons, and τ_h candidates from SM processes being misidentified as τ_h^{dis} candidates is estimated from simulation to be negligible, i.e., with an event yield lower than 0.1 across all bins defined in Table 2, because of the requirements on veto-electrons and

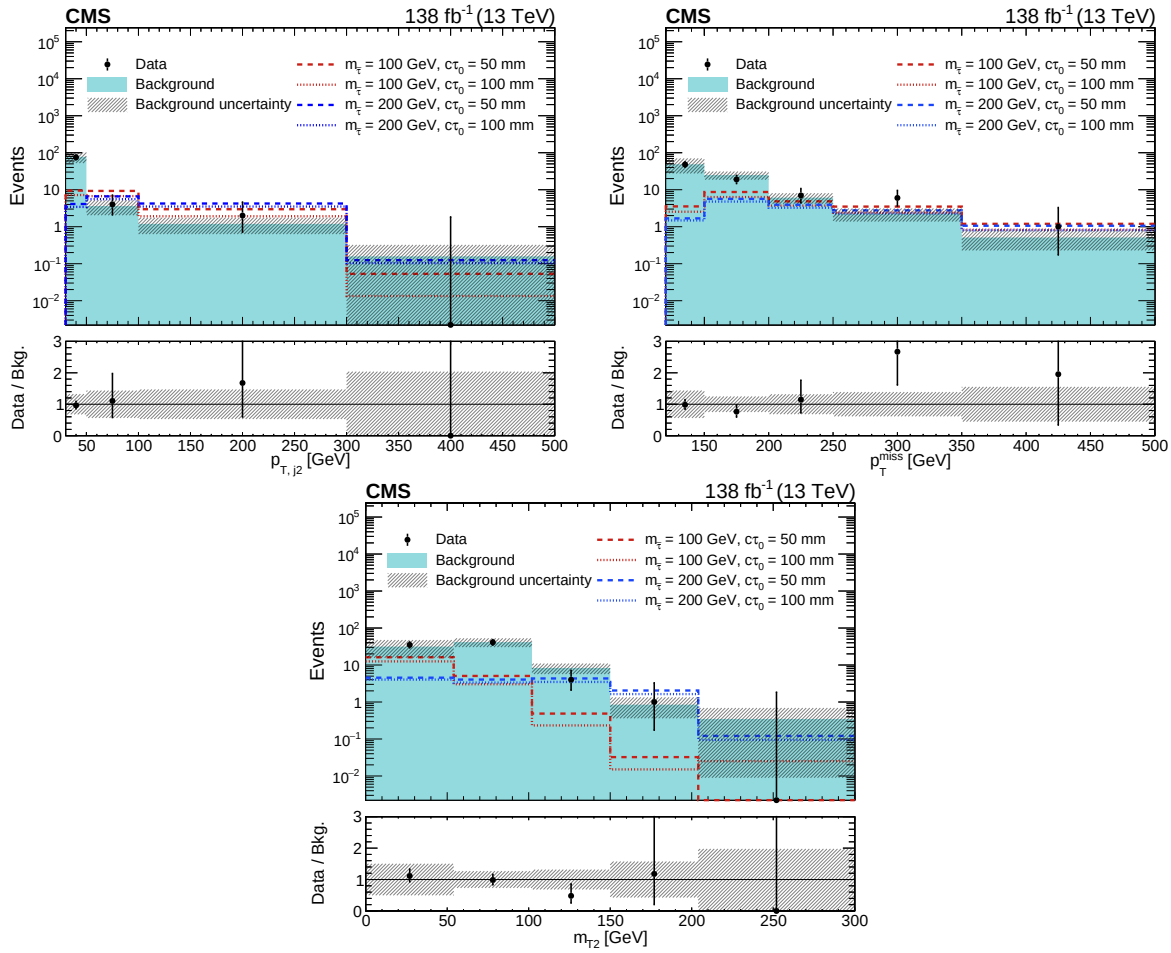

Figure 4: Distributions of the variables used to define the signal region for data and the predicted background: $p_{\mathrm{T,j2}}$ (upper left), $p_{\mathrm{T}}^{\mathrm{miss}}$ (upper right), and m_{T2} (lower). The signal distributions expected in the maximally mixed scenario for four representative sets of ($m_{\tilde{\tau}}$ [GeV], $c\tau_0$ [mm]) values are overlaid: (100, 50), (100, 100), (200, 50), and (200, 100). In bins where the observed yield is zero, the Garwood interval at 68% CL is shown as a positive uncertainty. The lower panel indicates the ratio of the observed number of events to the total predicted number of background events. The shaded bands indicate the statistical and systematic uncertainties in the predicted backgrounds, added in quadrature. The last bin includes the overflow.

veto-muons, and on the d_{xy} of the jets, as described in Sections 4.1 and 5. Therefore, they are not included in the background estimation.

Simulated samples are not suitable for estimating the misidentified-jet background from SM processes owing to the limited number of events entering the SR, especially in the tails of the search variable distributions presented in Section 5. Therefore, we employ a technique fully based on control samples in data for evaluating the SM background arising from jets that are misidentified as $\tau_{\mathrm{h}}^{\mathrm{dis}}$ candidates. The procedure has been developed by combining the strategies used in Refs. [36, 97, 98]. In order to describe the method, the following quantities are to be considered:

- Misidentification probability f, defined as the probability of a jet passing WPT, pro-

vided it has passed WPL:

$$f = n_{\text{jet}}(\text{WPT})/n_{\text{jet}}(\text{WPL}). \tag{4}$$

The probability of a jet passing WPL but failing WPT is then $1 - f$.

- N: total number of events where exactly two jets pass WPL.
- N_{T0}, N_{T1}, and N_{T2}: number of events satisfying T0, T1, and T2 criteria, respectively, as described in Table 1.

Noting the above definitions, the following equations can be established:

$$N_{\text{T0}} = (1 - f_1)(1 - f_2)N, \tag{5a}$$
$$N_{\text{T1}} = [f_1(1 - f_2) + (1 - f_1)f_2]N, \tag{5b}$$
$$N_{\text{T2}} = f_1 f_2 N. \tag{5c}$$

Here f_1 and f_2 are the misidentification probabilities of the $\tau_{\text{h}}^{\text{dis}}$ candidate with higher and lower p_{T}, respectively. Taking the ratio between the subequations of Eq. (5), the following quantities can be obtained:

- Prediction of N_{T1} from N_{T0}:

$$N_{\text{T10}} \equiv N_{\text{T1}}^{\text{pred}} = \frac{f_1(1 - f_2) + (1 - f_1)f_2}{(1 - f_1)(1 - f_2)} N_{\text{T0}}. \tag{6}$$

- Prediction of N_{T2} from N_{T0}:

$$N_{\text{T20}} \equiv N_{\text{T2}}^{\text{pred}} = \frac{f_1 f_2}{(1 - f_1)(1 - f_2)} N_{\text{T0}}. \tag{7}$$

- Prediction of N_{T2} from N_{T1}:

$$N_{\text{T21}} \equiv N_{\text{T2}}^{\text{pred}} = \frac{f_1 f_2}{f_1(1 - f_2) + (1 - f_1)f_2} N_{\text{T1}}. \tag{8}$$

Equation (4) is used to measure the misidentification probability f_{W} from data, in the WCR described in Section 5. An alternate measurement, f_{DY}, is performed in the DYCR in data as a cross-check, and is found to agree with f_{W} within the statistical uncertainties.

The misidentified-jet background predictions in BRT1 and the SR are obtained using f_{W} parametrized in two dimensions, in bins of p_{T} (30–40, 40–50, 50–70, 70–120, and >120 GeV) and $|d_{xy}|$ (0.2–0.5, 0.5–1, 1–2, 2–4, 4–10, 10–20, and >20 cm) of the jet. Their values are, approximately, in the 10–20 and 5–10 (5–10 and 30–40)% ranges with increasing p_{T} ($|d_{xy}|$), depending on the data-taking period.

Jets with large d_{xy} can have a degraded p_{T} resolution as the displacement of the tracks from the primary vertex can affect the measurement of their transverse momenta. Such jets would increase the $p_{\text{T}}^{\text{miss}}$ in the event, potentially causing the event to fail the m_{T} requirement used to select the WCR. This effect would induce a downward bias in the measured value of f_{W}, as the contribution from jets with large d_{xy} would be underestimated. To test the impact of this possible bias, the measurement of f_{W} is also performed in the WCR, without imposing the aforementioned selection on m_{T}. Additional measurements of f_{W} are performed in two subregions of this modified WCR, one with $50 \leq p_{\text{T}}^{\text{miss}} < 120$ GeV, and the other with $p_{\text{T}}^{\text{miss}} \geq$

120 GeV. These estimates of f_W obtained without the m_T requirement are found to be consistent with the nominal measurement reported above within the statistical uncertainties, even in the bins populated by jets with high p_T or large d_{xy}. This indicates that the potential bias from this effect is negligible.

We use BRT1 as the primary region for validating the background estimation as it is adjacent to the SR, while having a negligible signal contamination of $\lesssim$1%, compared to the predicted background. Figure 5 shows the observed event yields in BRT1 compared with the signal and background predictions, the latter (obtained using N_{T10}) being found to be consistent with the observed data. Additional validations are performed by using f_W (f_{DY}) to predict the yields in DYCRT1 and DYCRT2 (WCRT1 and WCRT2) and comparing them with the observed data in the corresponding regions. These comparisons are also found to agree within the uncertainties.

The primary background prediction in the SR is obtained using N_{T21} (Eq. 8). An alternate measurement is performed using N_{T20} (Eq. 7), serving as a cross-check against potential signal contamination in BRT1, which would have an impact on the estimation of N_{T21}. The two estimates are found to agree within uncertainties, and the difference between them is propagated as a systematic uncertainty, as reported in Section 7.

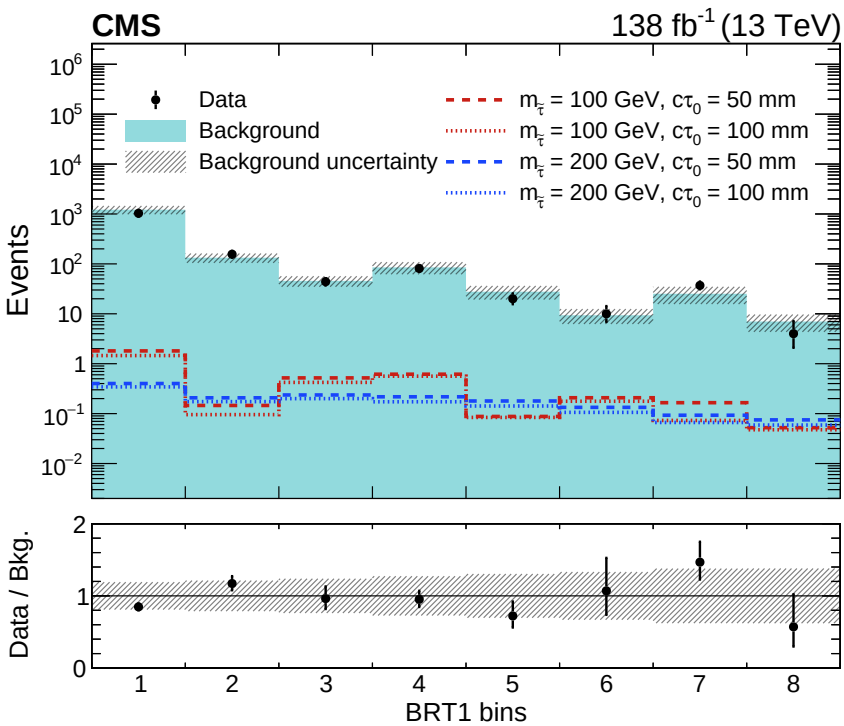

Figure 5: Observed and predicted event yields in the eight BRT1 bins, as defined in Table 2. The signal yields expected in the maximally mixed scenario for four representative sets of ($m_{\tilde{\tau}}$ [GeV], $c\tau_0$ [mm]) values are overlaid: (100, 50), (100, 100), (200, 50), and (200, 100). The lower panel indicates the ratio of the observed number of events to the total predicted number of background events in each bin. The shaded bands indicate the statistical and systematic uncertainties in the background, added in quadrature.

7 Systematic uncertainties

Several sources of systematic uncertainties affecting the prediction of both signal and background yields are taken into account, and their contributions are summarized in Table 3.

Table 3: Relative systematic uncertainties expressed as a percentage (%) of the signal and background yields in the SR, from various sources considered in this search, after accounting for their correlations between the data-taking periods. The three values correspond to the minimum, median, and maximum values across the eight SR bins, as defined in Table 2. For cases where the minimum and maximum values differ by less than 1, only the median is shown. In the header row, $m_{\tilde{\tau}}$ and $c\tau_0$ are in units of GeV and mm, respectively. The uncertainty values shown here are prior to the maximum likelihood fit described in Section 8.

Uncertainty source	Background	$m_{\tilde{\tau}}(100)$ $c\tau_0(50)$	$m_{\tilde{\tau}}(100)$ $c\tau_0(100)$	$m_{\tilde{\tau}}(200)$ $c\tau_0(50)$	$m_{\tilde{\tau}}(200)$ $c\tau_0(100)$
Parton distribution function	—	3.5, 3.8, 6	2.9, 4.2, 6.4	4, 4.6, 5.9	3.9, 4.4, 5.2
μ_R scale	—	<0.1, 0.29, 1.4	<0.1, 0.46, 1.3	<0.1	0.1
μ_F scale	—	0.62, 4.3, 7.1	1.3, 5.1, 7.1	0.63, 1.1, 2.9	0.65, 0.94, 2.8
Jet energy scale	—	0.83, 2.4, 7.4	0.68, 3.2, 10	0.39, 1.4, 2.5	0.47, 1.1, 2.5
Jet energy resolution	—	0.19, 0.54, 7.4	0.14, 0.82, 4.3	0.22	0.17
p_T^{miss} unclustered energy	—	0.26, 0.9, 7.4	0.31, 1.1, 8.9	0.28	0.33
Pileup	—	0.66, 1.2, 3.3	0.62, 0.98, 5.1	0.61	0.59
Integrated luminosity	—	1.7	1.7	1.7	1.7
p_T^{miss} trigger	—	1.6, 16, 20	1.6, 15, 20	1.7, 14, 16	1.6, 14, 16
DISTAU identification	—	17, 18, 19	17, 18, 19	17	18
Misid. probability estimation region	11, 11, 13	—	—	—	—
Misid. probability sample size	15, 30, 57	—	—	—	—
Alternative bkg. prediction	8.5, 24, 53	—	—	—	—
Bkg. correction from BRT1	2.8, 5.2, 8.1	—	—	—	—

Sources of theoretical uncertainties affecting the signal simulation include the PDFs and missing higher-order corrections. The effect of these are estimated from the variation in signal yields from alternate PDF sets [57, 58, 99], and from independently varying the factorization (μ_F) and renormalization (μ_R) scales up and down by a factor of two with the constraint $0.5 \leq (\mu_R/\mu_F) \leq 2$ to account for the uncertainty arising from missing higher-order corrections. The SYSCALC package [100] is used for this purpose.

The experimental sources affecting the signal include the jet energy scale and jet energy resolution, the effect of unclustered energy in calculating p_T^{miss}, pileup reweighting, integrated luminosity, and the uncertainty in the modeling of the p_T^{miss} trigger. The last uncertainty is taken to be the difference from unity of the simulation-to-data correction to the trigger efficiency for events with $p_T^{miss} < 250\,\text{GeV}$, estimated with events selected by a single-muon trigger. This uncertainty is larger than the statistical uncertainty in the correction factor in this p_T^{miss} region, and is intended to account for potential mismodeling of the trigger efficiency turn-on curve in simulation. For events with higher p_T^{miss}, i.e. in the plateau region of the trigger efficiency, the statistical uncertainty in the correction factor is used. The simulation is reweighted to make its pileup vertex distribution identical to that of the data. The uncertainty in estimating the number of pileup interactions is estimated by varying the total inelastic cross section by $\pm 4.6\%$ [101].

This is propagated as an uncertainty in the pileup reweighting factor applied to the simulation. The uncertainty in the measured integrated luminosity amounts to 1.2, 2.3, and 2.5% in 2016, 2017, and 2018 [102–104], respectively. In addition, the uncertainty in the correction factor for the DISTAU identification efficiency described in Section 4.2, is also taken into account.

All sources of systematic uncertainties affecting the signal are considered uncorrelated across data-taking years, except for those from theory and the integrated luminosity uncertainty. The theory uncertainties are treated as fully correlated across the years, and the integrated luminosity uncertainty is treated as partially correlated, which results in a value of 1.7% on combining the years.

The following systematic uncertainties are propagated to the prediction of the final background yields. They are discussed here in the order of their appearance in Table 3.

Since the predicted background in the BR is obtained using f_{W}, which is measured in a W+jets enriched region, one needs to account for how differences between WCR and BR can impact the extrapolation of the misidentification probability in the BR (f_{BR}). These can arise from differences between the two regions in the flavor composition of the parton corresponding to the jet that is misidentified as a $\tau_{\mathrm{h}}^{\mathrm{dis}}$ candidate. We use simulations of the SM processes described in Section 3 to estimate the relative difference $|f_{\mathrm{W}}^{\mathrm{MC}} - f_{\mathrm{BR}}^{\mathrm{MC}}|/f_{\mathrm{W}}^{\mathrm{MC}}$, which is found to be about 10%. This is treated as an uncertainty in f_{W} (labeled "Misid. probability estimation region") correlated across data-taking years and propagated to the background prediction. The statistical uncertainty in f_{W} due to the finite size of the WCR (labeled "Misid. probability sample size") is also propagated to the prediction of the background yields. In addition, the difference between the primary and alternate background predictions, as discussed in Section 6 is taken as an uncertainty (labeled "Alternative bkg. prediction"). These last two sources of uncertainties are treated as uncorrelated across data-taking years.

The observed data in the BRT1 region for the first $19\,\mathrm{fb}^{-1}$ of 2016 data taking were observed to be lower than the estimated background by a factor of 0.7 uniformly across all bins. The discrepancy can possibly be attributed to the saturation effects observed in the APV25 readout chip preamplifier used in the tracker [105], during the same data-taking period. Therefore, an additional correction of 0.7 ± 0.3 is applied to the SR in that portion of the data set, with the uncertainty ("Bkg. correction from BRT1") being taken as the deviation of the factor from unity. This correction has a negligible effect on the final results described in Section 8.

8 Results

The observed and expected yields along with their uncertainties in all eight SR bins are shown in Table 4 and Fig. 6, along with four representative signal hypotheses. The number of events observed in data is found to be consistent with the SM background prediction.

The test statistic used for the interpretation of the result is the LHC-style profile likelihood ratio $q_r = -2\ln(\mathcal{L}_r/\mathcal{L}_{\mathrm{max}})$, where $\mathcal{L}_r$ is the maximum likelihood for a fixed signal strength modifier r, and $\mathcal{L}_{\mathrm{max}}$ is the global maximum of the likelihood [106]. The systematic uncertainties discussed in Section 7 are modeled by log-normal distributions [106] in the likelihood function. We set upper limits on signal production cross section at 95% CL using a modified frequentist approach with a $\mathrm{CL_s}$ criterion [107, 108], with test-statistic distributions obtained from ensembles of pseudo-experiments. In this calculation, all the background and signal uncertainties are incorporated as nuisance parameters and profiled in the maximum likelihood fit [106].

The final results are obtained by simultaneously fitting all the SR bins from the 2016, 2017,

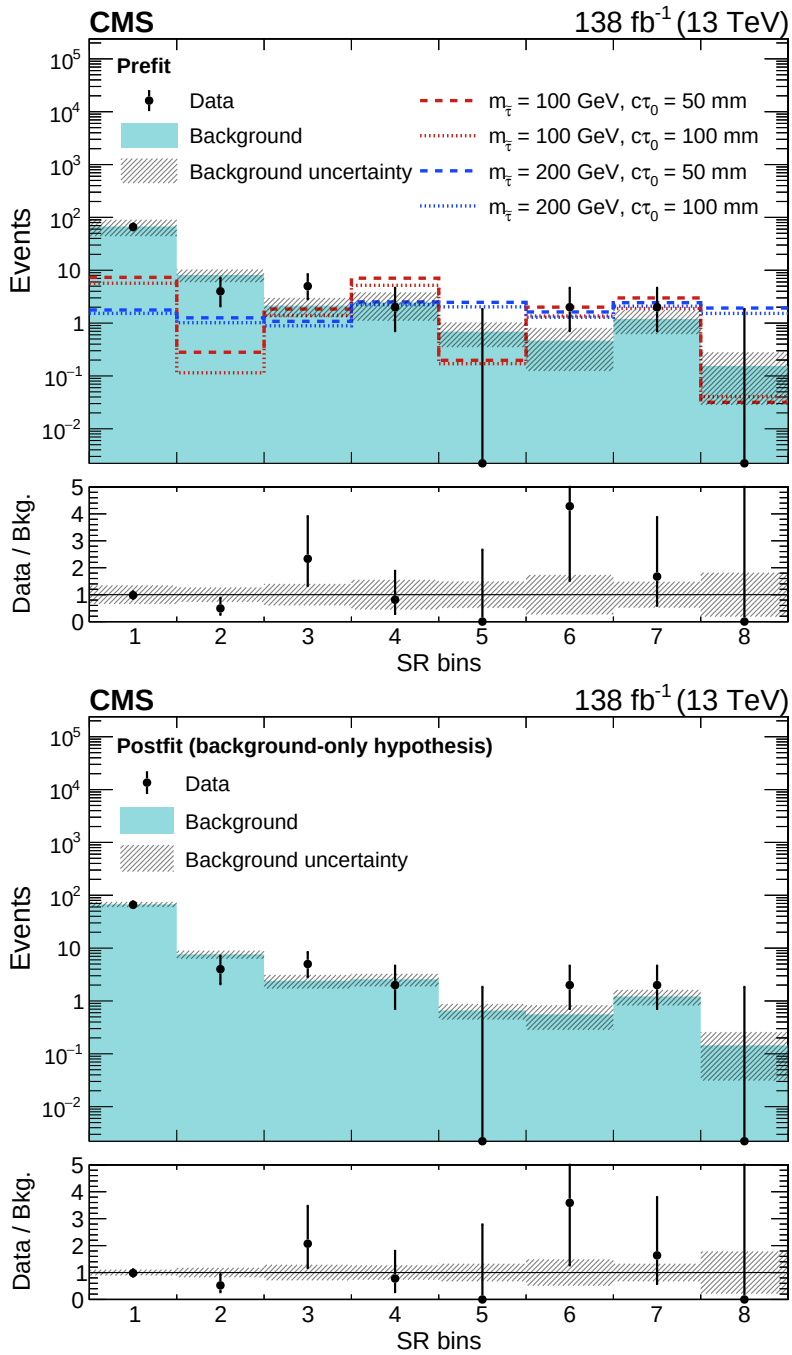

Figure 6: Observed and predicted event yields in the eight SR bins as defined in Table 2. The signal yields expected in the maximally mixed scenario for four representative sets of ($m_{\tilde{\tau}}$ [GeV], $c\tau_0$ [mm]) values are overlaid: (100, 50), (100, 100), (200, 50), and (200, 100). In bins where the observed yield is zero, the Garwood interval at 68% CL is shown as a positive uncertainty. The lower panel indicates the ratio of the observed number of events to the total predicted number of background events in each bin. The shaded bands indicate the statistical and systematic uncertainties in the background prediction, added in quadrature. The predicted yields and uncertainties shown in the upper (lower) panel are before (after) the maximum likelihood fit to data under the background-only hypothesis, as described in Section 8.

Table 4: Predicted background and signal yields in the eight SR bins, as defined in Table 2, are shown alongside the background yields obtained from the maximum likelihood fit to data under the background-only hypothesis and the number of events observed in the recorded data. All yields, except for the number of recorded events, are quoted with uncertainties obtained by adding statistical and systematic components in quadrature. Signal and predicted background uncertainties correspond to the prefit values, while the postfit background uncertainties are taken from the fit described in Section 8. In the header row, $m_{\widetilde{\tau}}$ and $c\tau_0$ are in units of GeV and mm, respectively.

SR bin	Data	Bkg. (prefit)	Bkg. (postfit)	$m_{\widetilde{\tau}}(100)$ $c\tau_0(50)$	$m_{\widetilde{\tau}}(100)$ $c\tau_0(100)$	$m_{\widetilde{\tau}}(200)$ $c\tau_0(50)$	$m_{\widetilde{\tau}}(200)$ $c\tau_0(100)$
1	66	67±23	67±8	7.3±1.8	5.7±1.4	1.8±0.4	1.5±0.4
2	4	8.1±2.2	7.6±1.4	0.28±0.09	0.11±0.04	1.26±0.29	1.02±0.23
3	5	2.1±0.9	2.4±0.7	1.8±0.4	1.39±0.30	1.08±0.21	0.89±0.17
4	2	2.5±1.3	2.6±0.7	7.1±1.8	5.2±1.3	2.5±0.6	2.2±0.5
5	0	0.7±0.4	0.66±0.22	0.20±0.06	0.17±0.06	2.5±0.6	2.0±0.5
6	2	0.47±0.34	0.56±0.25	2.0±0.4	1.36±0.30	1.62±0.31	1.29±0.25
7	2	1.2±0.6	1.2±0.4	3.0±0.7	1.9±0.5	2.4±0.5	2.1±0.5
8	0	0.15±0.13	0.14±0.10	0.032±0.015	0.041±0.017	1.9±0.4	1.5±0.4
Tot.	81	83±27	83±11	22±5	16±4	15.1±3.3	12.6±2.8

and 2018 data sets, using the CMS statistical analysis and combination tool COMBINE [109]. Figure 7 shows the observed and expected exclusion limits for the pair production of long-lived staus decaying to a τ lepton and a nearly massless gravitino ($m_{\widetilde{G}} = 1$ GeV) in the plane of the stau mass and the proper decay length. In the maximally mixed scenario, the observed (expected) range of excluded $m_{\widetilde{\tau}}$ values is 126–260 (90–335) GeV for $c\tau_0 = 50$ mm, and the observed (expected) range of excluded $c\tau_0$ values is 21–94 (12–169) mm for $m_{\widetilde{\tau}} = 200$ GeV. In the mass-degenerate scenario, the observed (expected) range of excluded $m_{\widetilde{\tau}}$ values is 90–425 (90–491) GeV for $c\tau_0 = 50$ mm, and the observed (expected) range of excluded $c\tau_0$ values is 6–333 (5.5–442) mm for $m_{\widetilde{\tau}} = 200$ GeV. The exclusion limits in the mass-degenerate scenario are stronger than in the maximally mixed scenario, as the former has a larger cross section from the production of both $\widetilde{\tau}_1$ and $\widetilde{\tau}_2$, as discussed in Section 3. Upper limits on the cross section as functions of $m_{\widetilde{\tau}}$ are presented in Figs. 8 and 9, for maximally mixed and mass-degenerate scenarios, respectively.

As reported in Table 4 and Fig. 6, the predicted background is lower than the observed yield by approximately one standard deviation in bin 6. Since bin 6 corresponds to an intermediate range of $p_{\mathrm{T,j2}}$ (50–100 GeV), high $p_{\mathrm{T}}^{\mathrm{miss}}$ (>250 GeV), and any value of m_{T2}, it is sensitive to a broad range of $m_{\widetilde{\tau}}$ and $c\tau_0$ signal hypotheses. This results in the observed limits being weaker than the expected ones by approximately one standard deviation, across all tested hypotheses in the plane of $m_{\widetilde{\tau}}$ and $c\tau_0$.

The upper limits on the production cross section become weaker for $c\tau_0$ below about 10 mm, as the $\tau_{\mathrm{h}}^{\mathrm{dis}}$ candidates have smaller displacements and resemble background jets. For $c\tau_0$ above a few hundred millimeters, the stau decays in the outer layers of the tracker, which reduces the

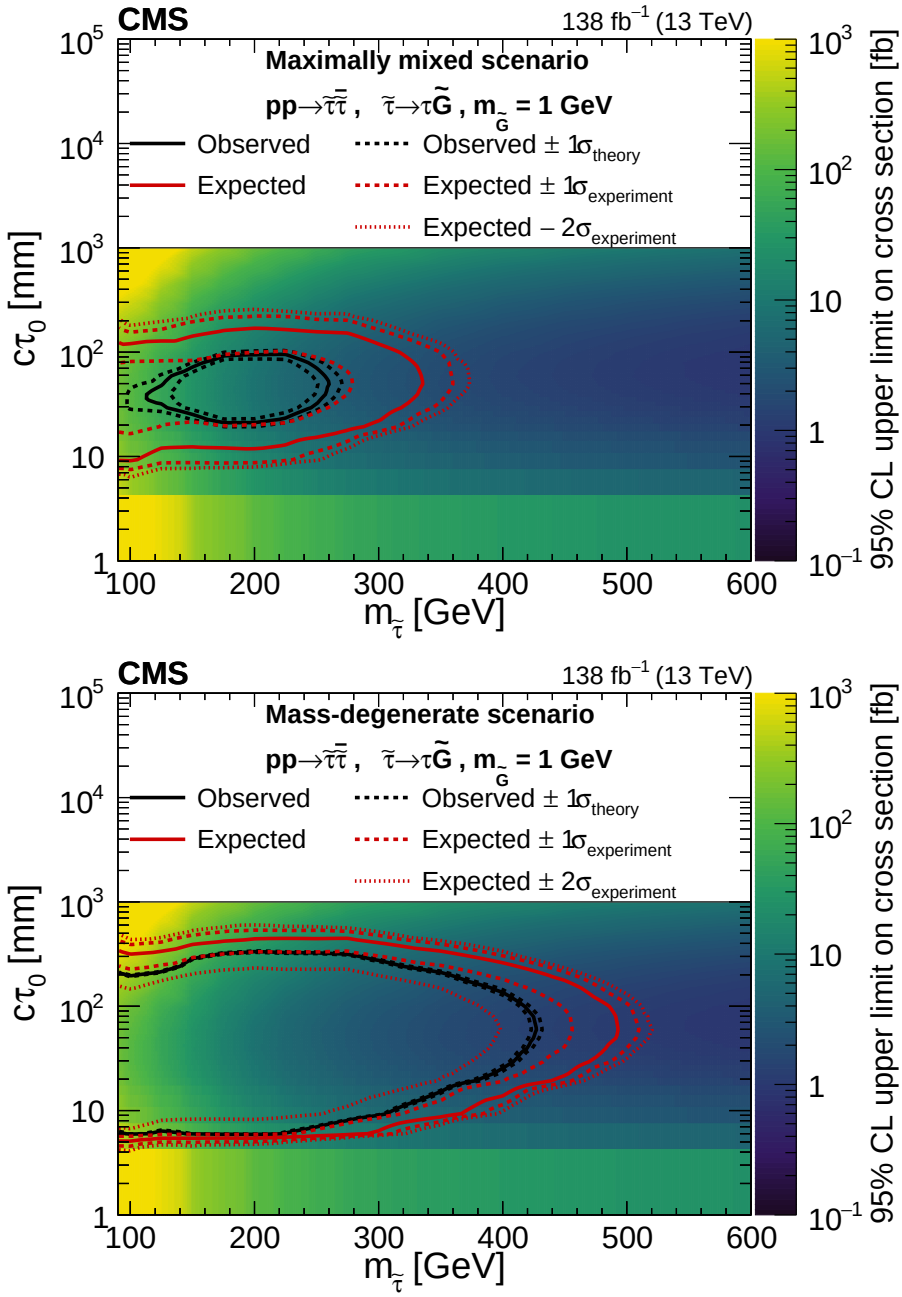

Figure 7: Exclusion limits at 95% CL for the pair production of long-lived staus decaying to a τ lepton and a nearly massless gravitino ($m_{\tilde{G}} = 1$ GeV), displayed in the plane of $m_{\tilde{\tau}}$ and $c\tau_0$. The maximally mixed (mass-degenerate) scenario is presented in the upper (lower) panel. The color axis represents the observed upper limit on the cross section. The signal cross sections are evaluated using NLO+NLL calculations. The black (red) lines represent the observed (expected) limits on $m_{\tilde{\tau}}$ and $c\tau_0$ and enclose the region excluded at 95% CL. The solid lines represent the central values. The dashed (dotted) red lines indicate the region containing 68% (95%) of the distribution of limits expected under the background-only hypothesis accounting for experimental uncertainties ($\sigma_{\text{experiment}}$). The red dotted line corresponding to "Expected+$2\sigma_{\text{experiment}}$" is not shown for the maximally mixed scenario, as it does not exclude any points in this plane. The dashed black lines show the change in the observed limit from the variation of the signal cross sections within their theoretical uncertainties (σ_{theory}).

reconstruction efficiency of $\tau_{\mathrm{h}}^{\mathrm{dis}}$ candidates as the charged pions from the decay of the τ lepton have fewer hits in the tracker. In addition, a stau with high $c\tau_0$ can produce a signature in the tracker similar to that of a $\tau_{\mathrm{h}}^{\mathrm{dis}}$ candidate with very small $|d_{xy}|$ or of a background jet. These effects result in a degradation of the upper limits at large values of $c\tau_0$. With growing $m_{\tilde{\tau}}$, there is a gain in signal event yields because of an increase in the momenta of the $\tau_{\mathrm{h}}^{\mathrm{dis}}$ candidates and the $p_{\mathrm{T}}^{\mathrm{miss}}$ in the events, which causes the upper limits to become more stringent.

The improvement in observed upper limits on the production cross section for $m_{\tilde{\tau}} = 300\,\mathrm{GeV}$ in the mass-degenerate scenario ranges from a factor of 5.7 at $c\tau_0 = 3\,\mathrm{mm}$ to 2.5 at $c\tau_0 = 300\,\mathrm{mm}$, compared to the best available limits at $\sqrt{s} = 13\,\mathrm{TeV}$ reported in the search for long-lived staus in Ref. [35]. The improvement in the observed (expected) exclusion limits is also significant, for example, the maximum excluded $\tilde{\tau}$ mass reaches 425 GeV (490 GeV) at $c\tau_0 = 50\,\mathrm{mm}$, compared to 330 GeV (315 GeV) in Ref. [35]. The range of excluded $\tilde{\tau}$ masses in this search is similar to that in Ref. [40], which also includes data collected at $\sqrt{s} = 13.6\,\mathrm{TeV}$. However, the range of excluded $c\tau_0$ values at low $\tilde{\tau}$ masses in Ref. [40] is wider (3–1200 mm at $m_{\tilde{\tau}} = 100\,\mathrm{GeV}$) than that in the present search (6–200 mm at $m_{\tilde{\tau}} = 100\,\mathrm{GeV}$) owing to the usage of novel triggers for reconstructing displaced tracks with low momentum. The results are also complementary to some previous searches, e.g. the search described in Ref. [36], which explored small lifetimes ($c\tau_0 < 2.5\,\mathrm{mm}$) for the maximally mixed scenario, and the one described in Ref. [39], which targeted long lifetimes ($c\tau_0 > 900\,\mathrm{mm}$) for the mass-degenerate scenario.

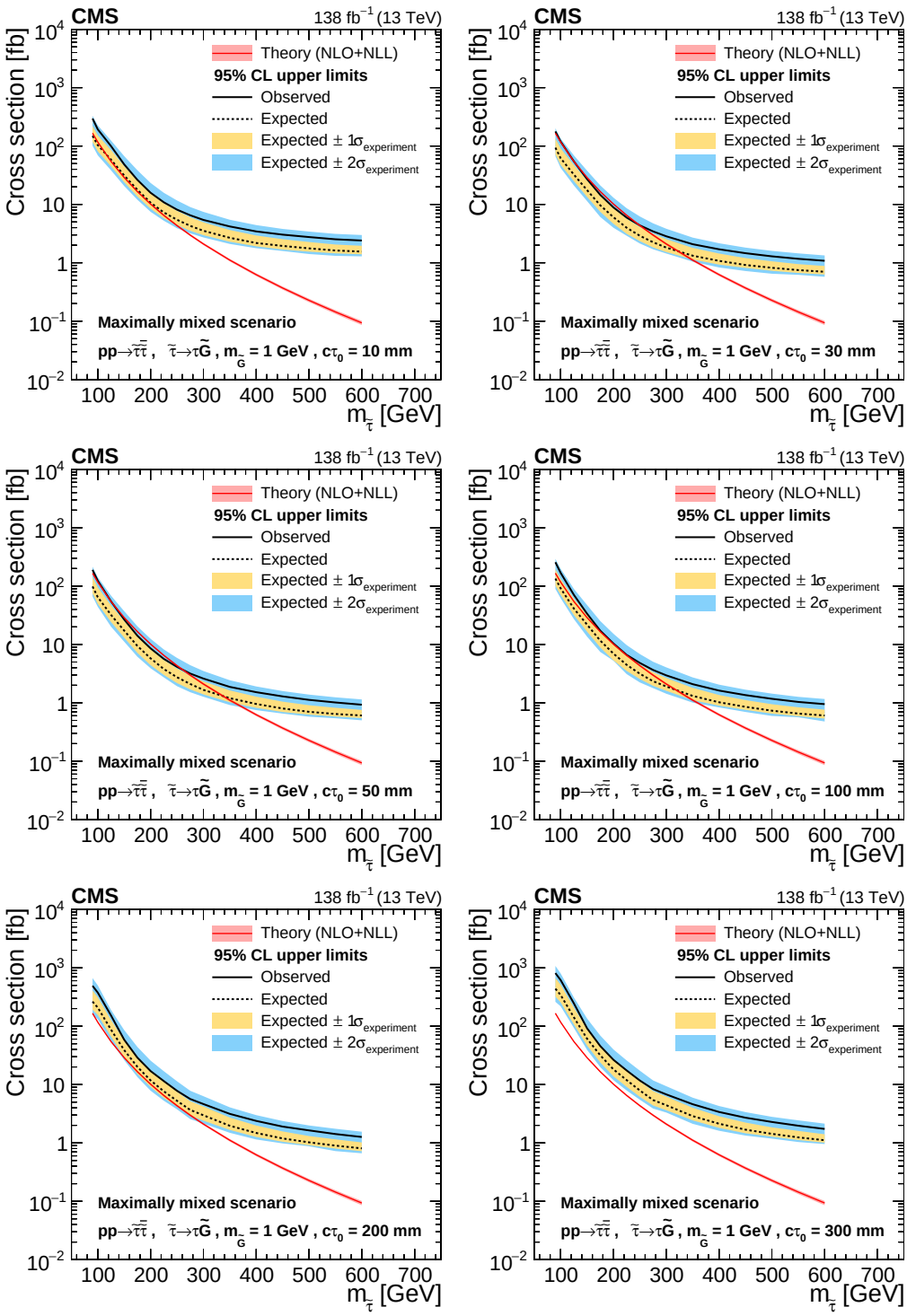

Figure 8: Cross section upper limits at 95% CL for the pair production of long-lived staus decaying to a τ lepton and a nearly massless gravitino ($m_{\tilde{G}} = 1$ GeV) in the maximally mixed scenario, as a function of $m_{\tilde{\tau}}$, for $c\tau_0 = 10$, 30, 50, 100, 200, and 300 mm (left to right, upper to lower). The inner (yellow) and outer (blue) bands indicate the regions containing 68 and 95%, respectively, of the distribution of limits expected under the background-only hypothesis. The central values of the expected upper limits are denoted by the dashed black line. The solid black line represents the observed upper limits. The signal cross sections and uncertainties evaluated using NLO+NLL calculations are shown as a red line and shaded band.

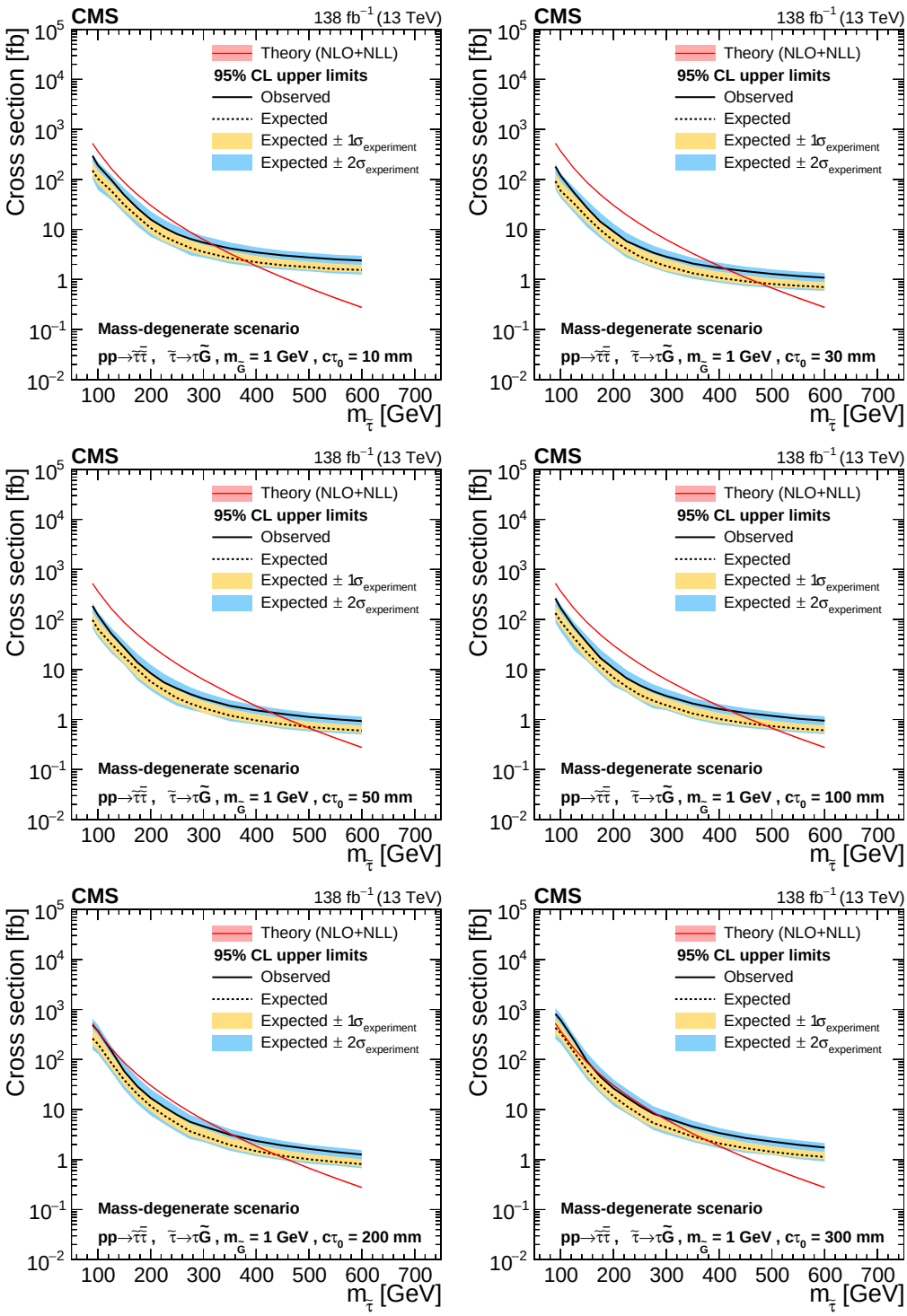

Figure 9: Cross section upper limits at 95% CL for the pair production of long-lived staus decaying to a τ lepton and a nearly massless gravitino ($m_{\tilde{G}} = 1$ GeV) in the mass-degenerate scenario, as a function of $m_{\tilde{\tau}}$, for $c\tau_0 = 10$, 30, 50, 100, 200, and 300 mm (left to right, upper to lower). The inner (yellow) and outer (blue) bands indicate the regions containing 68 and 95%, respectively, of the distribution of limits expected under the background-only hypothesis. The central values of the expected upper limits are denoted by the dashed black line. The solid black line represents the observed upper limits. The signal cross sections and uncertainties evaluated using NLO+NLL calculations are shown as a red line and shaded band.

9 Summary

A search for the direct pair production of long-lived superpartners of the tau lepton (staus) has been performed in final states with two hadronically decaying tau leptons (τ_h) using data collected by the CMS detector in 2016–2018, corresponding to an integrated luminosity of 138 fb^{-1}. The potentially large background from misidentified jets in the fully hadronic final state is efficiently suppressed by the DisTau neural network algorithm, specifically designed to identify displaced τ_h candidates. In the maximally mixed (mass-degenerate) scenario, stau masses, $m_{\tilde{\tau}}$, in the 126–260 (90–425) GeV range are excluded for a proper decay length, $c\tau_0$, of 50 mm, and stau proper decay lengths in the range 21–94 (6–333) mm are excluded for $m_{\tilde{\tau}} = 200$ GeV. The development of a dedicated algorithm targeting displaced τ_h signatures has led to a significant improvement in the experimental sensitivity. These results improve the exclusion limits compared to previous searches [33–39] at $\sqrt{s} = 13$ TeV, and extend the parameter space explored in the context of supersymmetry.

Acknowledgments

We congratulate our colleagues in the CERN accelerator departments for the excellent performance of the LHC and thank the technical and administrative staffs at CERN and at other CMS institutes for their contributions to the success of the CMS effort. In addition, we gratefully acknowledge the computing centers and personnel of the Worldwide LHC Computing Grid and other centers for delivering so effectively the computing infrastructure essential to our analyses. Finally, we acknowledge the enduring support for the construction and operation of the LHC, the CMS detector, and the supporting computing infrastructure provided by the following funding agencies: SC (Armenia), BMBWF and FWF (Austria); FNRS and FWO (Belgium); CNPq, CAPES, FAPERJ, FAPERGS, and FAPESP (Brazil); MES and BNSF (Bulgaria); CERN; CAS, MoST, and NSFC (China); MINCIENCIAS (Colombia); MSES and CSF (Croatia); RIF (Cyprus); SENESCYT (Ecuador); ERC PRG, TARISTU24-TK10 and MoER TK202 (Estonia); Academy of Finland, MEC, and HIP (Finland); CEA and CNRS/IN2P3 (France); SRNSF (Georgia); BMFTR, DFG, and HGF (Germany); GSRI (Greece); NKFIH (Hungary); DAE and DST (India); IPM (Iran); SFI (Ireland); INFN (Italy); MSIT and NRF (Republic of Korea); MES (Latvia); LMTLT (Lithuania); MOE and UM (Malaysia); BUAP, CINVESTAV, CONACYT, LNS, SEP, and UASLP-FAI (Mexico); MOS (Montenegro); MBIE (New Zealand); PAEC (Pakistan); MES, NSC, and NAWA (Poland); FCT (Portugal); MESTD (Serbia); MICIU/AEI and PCTI (Spain); MOSTR (Sri Lanka); Swiss Funding Agencies (Switzerland); MST (Taipei); MHESI (Thailand); TUBITAK and TENMAK (Türkiye); NASU (Ukraine); STFC (United Kingdom); DOE and NSF (USA).

Individuals have received support from the Marie-Curie program and the European Research Council and Horizon 2020 Grant, contract Nos. 675440, 724704, 752730, 758316, 765710, 824093, 101115353, 101002207, 101001205, and COST Action CA16108 (European Union); the Leventis Foundation; the Alfred P. Sloan Foundation; the Alexander von Humboldt Foundation; the Science Committee, project no. 22rl-037 (Armenia); the Fonds pour la Formation à la Recherche dans l'Industrie et dans l'Agriculture (FRIA) and Fonds voor Wetenschappelijk Onderzoek contract No. 1228724N (Belgium); the Beijing Municipal Science & Technology Commission, No. Z191100007219010, the Fundamental Research Funds for the Central Universities, the Ministry of Science and Technology of China under Grant No. 2023YFA1605804, the Natural Science Foundation of China under Grant No. 12535004, and USTC Research Funds of the Double First-Class Initiative No. YD2030002017 (China); the Ministry of Education, Youth and Sports (MEYS) of the Czech Republic; the Shota Rustaveli National Science Foundation, grant FR-22-

985 (Georgia); the Deutsche Forschungsgemeinschaft (DFG), among others, under Germany's Excellence Strategy – EXC 2121 "Quantum Universe" – 390833306, and under project number 400140256 - GRK2497; the Hellenic Foundation for Research and Innovation (HFRI), Project Number 2288 (Greece); the Hungarian Academy of Sciences, the New National Excellence Program - ÚNKP, the NKFIH research grants K 131991, K 133046, K 138136, K 143460, K 143477, K 146913, K 146914, K 147048, 2020-2.2.1-ED-2021-00181, TKP2021-NKTA-64, and 2025-1.1.5-NEMZ_KI-2025-00004 (Hungary); the Council of Science and Industrial Research, India; ICSC – National Research Center for High Performance Computing, Big Data and Quantum Computing, FAIR – Future Artificial Intelligence Research, and CUP I53D23001070006 (Mission 4 Component 1), funded by the NextGenerationEU program (Italy); the Latvian Council of Science; the Ministry of Education and Science, project no. 2022/WK/14, and the National Science Center, contracts Opus 2021/41/B/ST2/01369, 2021/43/B/ST2/01552, 2023/49/B/ST2/03273, and the NAWA contract BPN/PPO/2021/1/00011 (Poland); the Fundação para a Ciência e a Tecnologia, grant CEECIND/01334/2018 (Portugal); the National Priorities Research Program by Qatar National Research Fund; MICIU/AEI/10.13039/501100011033, ERDF/EU, "European Union NextGenerationEU/PRTR", and Programa Severo Ochoa del Principado de Asturias (Spain); the Chulalongkorn Academic into Its 2nd Century Project Advancement Project, the National Science, Research and Innovation Fund program IND_FF_68_369_2300_097, and the Program Management Unit for Human Resources & Institutional Development, Research and Innovation, grant B39G680009 (Thailand); the Kavli Foundation; the Nvidia Corporation; the SuperMicro Corporation; the Welch Foundation, contract C-1845; and the Weston Havens Foundation (USA).

References

[1] P. Ramond, "Dual theory for free fermions", *Phys. Rev. D* **3** (1971) 2415, doi:10.1103/PhysRevD.3.2415.

[2] Yu. A. Golfand and E. P. Likhtman, "Extension of the algebra of Poincaré group generators and violation of p invariance", *JETP Lett.* **13** (1971) 323, doi:10.1142/9789814542340_0001.

[3] A. Neveu and J. H. Schwarz, "Factorizable dual model of pions", *Nucl. Phys. B* **31** (1971) 86, doi:10.1016/0550-3213(71)90448-2.

[4] D. V. Volkov and V. P. Akulov, "Possible universal neutrino interaction", *JETP Lett.* **16** (1972) 438.

[5] J. Wess and B. Zumino, "A Lagrangian model invariant under supergauge transformations", *Phys. Lett. B* **49** (1974) 52, doi:10.1016/0370-2693(74)90578-4.

[6] J. Wess and B. Zumino, "Supergauge transformations in four dimensions", *Nucl. Phys. B* **70** (1974) 39, doi:10.1016/0550-3213(74)90355-1.

[7] P. Fayet, "Supergauge invariant extension of the Higgs mechanism and a model for the electron and its neutrino", *Nucl. Phys. B* **90** (1975) 104, doi:10.1016/0550-3213(75)90636-7.

[8] H. P. Nilles, "Supersymmetry, supergravity and particle physics", *Phys. Rept.* **110** (1984) 1, doi:10.1016/0370-1573(84)90008-5.

[9] G. 't Hooft, "Naturalness, chiral symmetry, and spontaneous chiral symmetry breaking", *NATO Sci. Ser. B* **59** (1980) 135, doi:10.1007/978-1-4684-7571-5_9.

[10] E. Witten, "Dynamical breaking of supersymmetry", *Nucl. Phys. B* **188** (1981) 513, doi:10.1016/0550-3213(81)90006-7.

[11] M. Dine, W. Fischler, and M. Srednicki, "Supersymmetric technicolor", *Nucl. Phys. B* **189** (1981) 575, doi:10.1016/0550-3213(81)90582-4.

[12] S. Dimopoulos and S. Raby, "Supercolor", *Nucl. Phys. B* **192** (1981) 353, doi:10.1016/0550-3213(81)90430-2.

[13] S. Dimopoulos and H. Georgi, "Softly broken supersymmetry and SU(5)", *Nucl. Phys. B* **193** (1981) 150, doi:10.1016/0550-3213(81)90522-8.

[14] R. K. Kaul and P. Majumdar, "Cancellation of quadratically divergent mass corrections in globally supersymmetric spontaneously broken gauge theories", *Nucl. Phys. B* **199** (1982) 36, doi:10.1016/0550-3213(82)90565-X.

[15] ATLAS Collaboration, "Observation of a new particle in the search for the standard model Higgs boson with the ATLAS detector at the LHC", *Phys. Lett. B* **716** (2012) 1, doi:10.1016/j.physletb.2012.08.020, arXiv:1207.7214.

[16] CMS Collaboration, "Observation of a new boson at a mass of 125 GeV with the CMS experiment at the LHC", *Phys. Lett. B* **716** (2012) 30, doi:10.1016/j.physletb.2012.08.021, arXiv:1207.7235.

[17] CMS Collaboration, "Observation of a new boson with mass near 125 GeV in pp collisions at $\sqrt{s} = 7$ and 8 TeV", *JHEP* **06** (2013) 081, doi:10.1007/JHEP06(2013)081, arXiv:1303.4571.

[18] ATLAS Collaboration, "Measurement of the Higgs boson mass from the $\mathrm{H} \to \gamma\gamma$ and $\mathrm{H} \to \mathrm{ZZ}^* \to 4\ell$ channels with the ATLAS detector using 25 fb^{-1} of pp collision data", *Phys. Rev. D* **90** (2014) 052004, doi:10.1103/PhysRevD.90.052004, arXiv:1406.3827.

[19] CMS Collaboration, "Precise determination of the mass of the higgs boson and tests of compatibility of its couplings with the standard model predictions using proton collisions at 7 and 8 TeV", *Eur. Phys. J. C* **75** (2015) 212, doi:10.1140/epjc/s10052-015-3351-7, arXiv:1412.8662.

[20] ATLAS and CMS Collaborations, "Combined measurement of the Higgs boson mass in pp collisions at $\sqrt{s} = 7$ and 8 TeV with the ATLAS and CMS experiments", *Phys. Rev. Lett.* **114** (2015) 191803, doi:10.1103/PhysRevLett.114.191803, arXiv:1503.07589.

[21] G. R. Farrar and P. Fayet, "Phenomenology of the production, decay, and detection of new hadronic states associated with supersymmetry", *Phys. Lett. B* **76** (1978) 575, doi:10.1016/0370-2693(78)90858-4.

[22] C. Boehm, A. Djouadi, and M. Drees, "Light scalar top quarks and supersymmetric dark matter", *Phys. Rev. D* **62** (2000) 035012, doi:10.1103/PhysRevD.62.035012, arXiv:hep-ph/9911496.

[23] C. Balázs, M. Carena, and C. E. M. Wagner, "Dark matter, light stops and electroweak baryogenesis", *Phys. Rev. D* **70** (2004) 015007, doi:10.1103/PhysRevD.70.015007, arXiv:hep-ph/403224.

[24] G. Jungman, M. Kamionkowski, and K. Griest, "Supersymmetric dark matter", *Phys. Rept.* **267** (1996) 195, doi:10.1016/0370-1573(95)00058-5, arXiv:hep-ph/9506380.

[25] Particle Data Group, S. Navas et al., "Review of particle physics", *Phys. Rev. D* **110** (2024) 030001, doi:10.1103/PhysRevD.110.030001.

[26] G. F. Giudice and R. Rattazzi, "Theories with gauge mediated supersymmetry breaking", *Phys. Rept.* **322** (1999) 419, doi:10.1016/S0370-1573(99)00042-3, arXiv:hep-ph/9801271.

[27] P. Meade, N. Seiberg, and D. Shih, "General gauge mediation", *Prog. Theor. Phys. Suppl.* **177** (2009) 143, doi:10.1143/PTPS.177.143, arXiv:0801.3278.

[28] J. A. Evans and J. Shelton, "Long-lived staus and displaced leptons at the LHC", *JHEP* **04** (2016) 056, doi:10.1007/JHEP04(2016)056, arXiv:1601.01326.

[29] ALEPH Collaboration, "Search for scalar leptons in e^+e^- collisions at center-of-mass energies up to 209 GeV", *Phys. Lett. B* **526** (2002) 206, doi:10.1016/S0370-2693(01)01494-0, arXiv:hep-ex/0112011.

[30] DELPHI Collaboration, "Searches for supersymmetric particles in e^+e^- collisions up to 208 GeV and interpretation of the results within the MSSM", *Eur. Phys. J. C* **31** (2003) 421, doi:10.1140/epjc/s2003-01355-5, arXiv:hep-ex/0311019.

[31] L3 Collaboration, "Search for scalar leptons and scalar quarks at LEP", *Phys. Lett. B* **580** (2004) 37, doi:10.1016/j.physletb.2003.10.010, arXiv:hep-ex/0310007.

[32] OPAL Collaboration, "Search for anomalous production of dilepton events with missing transverse momentum in e+ e- collisions at $\sqrt{s} = 183$–209 GeV", *Eur. Phys. J. C* **32** (2004) 453, doi:10.1140/epjc/s2003-01466-y, arXiv:hep-ex/0309014.

[33] ATLAS Collaboration, "Search for direct stau production in events with two hadronic τ-leptons in $\sqrt{s} = 13$ TeV pp collisions with the ATLAS detector", *Phys. Rev. D* **101** (2020) 032009, doi:10.1103/PhysRevD.101.032009, arXiv:1911.06660.

[34] CMS Collaboration, "Search for direct pair production of supersymmetric partners to the τ lepton in proton-proton collisions at $\sqrt{s} = 13$ TeV", *Eur. Phys. J. C* **80** (2020) 189, doi:10.1140/epjc/s10052-020-7739-7, arXiv:1907.13179.

[35] ATLAS Collaboration, "Search for displaced leptons in $\sqrt{s} = 13$ TeV pp collisions with the ATLAS detector", *Phys. Rev. Lett.* **127** (2021) 051802, doi:10.1103/PhysRevLett.127.051802, arXiv:2011.07812.

[36] CMS Collaboration, "Search for direct pair production of supersymmetric partners of τ leptons in the final state with two hadronically decaying τ leptons and missing transverse momentum in proton-proton collisions at $\sqrt{s}$ = 13 TeV", *Phys. Rev. D* **108** (2023) 012011, doi:10.1103/PhysRevD.108.012011, arXiv:2207.02254.

[37] CMS Collaboration, "Search for long-lived particles decaying to leptons with large impact parameter in proton–proton collisions at $\sqrt{s} = 13$ TeV", *Eur. Phys. J. C* **82** (2022) 153, doi:10.1140/epjc/s10052-022-10027-3, arXiv:2110.04809.

[38] ATLAS Collaboration, "Search for electroweak production of supersymmetric particles in final states with two τ-leptons in $\sqrt{s}$ = 13 TeV pp collisions with the ATLAS detector", *JHEP* **05** (2024) 150, doi:10.1007/JHEP05(2024)150, arXiv:2402.00603.

[39] ATLAS Collaboration, "Search for long-lived charged particles using large specific ionisation loss and time of flight in 140 fb^{-1} of pp collisions at $\sqrt{s}$ = 13 TeV with the ATLAS detector", *JHEP* **07** (2025) 140, doi:10.1007/JHEP07(2025)140, arXiv:2502.06694.

[40] ATLAS Collaboration, "Search for displaced leptons in $\sqrt{s} = 13$ TeV and 13.6 TeV pp collisions with the ATLAS detector", *Phys. Rev. D* **112** (2025), no. 1, 012016, doi:10.1103/w8hh-xf24, arXiv:2410.16835.

[41] ATLAS Collaboration, "Search for the direct production of charginos, neutralinos and staus in final states with at least two hadronically decaying taus and missing transverse momentum in pp collisions at $\sqrt{s}$ = 8 TeV with the ATLAS detector", *JHEP* **10** (2014) 096, doi:10.1007/JHEP10(2014)096, arXiv:1407.0350.

[42] ATLAS Collaboration, "Search for the electroweak production of supersymmetric particles in $\sqrt{s} = 8$ TeV pp collisions with the ATLAS detector", *Phys. Rev. D* **93** (2016) 052002, doi:10.1103/PhysRevD.93.052002, arXiv:1509.07152.

[43] CMS Collaboration, "Search for electroweak production of charginos in final states with two τ leptons in pp collisions at $\sqrt{s} = 8$ TeV", *JHEP* **04** (2017) 018, doi:10.1007/JHEP04(2017)018, arXiv:1610.04870.

[44] CMS Collaboration, "Performance of reconstruction and identification of τ leptons decaying to hadrons and ν_τ in pp collisions at $\sqrt{s} = 13$ TeV", *JINST* **13** (2018) P10005, doi:10.1088/1748-0221/13/10/p10005, arXiv:1809.02816.

[45] CMS Collaboration, "Identification of hadronic tau lepton decays using a deep neural network", *JINST* **17** (2022) P07023, doi:10.1088/1748-0221/17/07/P07023, arXiv:2201.08458.

[46] CMS Collaboration, "Tau lepton identification in displaced topologies using machine learning at CMS", CMS Detector Performance Summary CMS-DP-2024-053, 2024.

[47] J. Alwall, P. Schuster, and N. Toro, "Simplified models for a first characterization of new physics at the LHC", *Phys. Rev. D* **79** (2009) 075020, doi:10.1103/PhysRevD.79.075020, arXiv:0810.3921.

[48] LHC New Physics Working Group, "Simplified models for LHC new physics searches", *J. Phys. G* **39** (2012) 105005, doi:10.1088/0954-3899/39/10/105005, arXiv:1105.2838.

[49] H. Qu and L. Gouskos, "Jet tagging via particle clouds", *Phys. Rev. D* **101** (2020) 056019, doi:10.1103/PhysRevD.101.056019, arXiv:1902.08570.

[50] HEPData record for this analysis, 2025. doi:10.17182/hepdata.166010.

[51] CMS Collaboration, "The CMS experiment at the CERN LHC", *JINST* **3** (2008) S08004, doi:10.1088/1748-0221/3/08/S08004.

[52] CMS Collaboration, "Development of the CMS detector for the CERN LHC Run 3", *JINST* **19** (2024) P05064, doi:10.1088/1748-0221/19/05/P05064, arXiv:2309.05466.

[53] CMS Collaboration, "Performance of the CMS level-1 trigger in proton-proton collisions at $\sqrt{s} = 13\,\text{TeV}$", *JINST* **15** (2020) P10017, doi:10.1088/1748-0221/15/10/P10017, arXiv:2006.10165.

[54] CMS Collaboration, "The CMS trigger system", *JINST* **12** (2017) P01020, doi:10.1088/1748-0221/12/01/P01020, arXiv:1609.02366.

[55] CMS Collaboration, "Performance of the CMS high-level trigger during LHC Run 2", *JINST* **19** (2024) P11021, doi:10.1088/1748-0221/19/11/P11021, arXiv:2410.17038.

[56] J. Alwall et al., "The automated computation of tree-level and next-to-leading order differential cross sections, and their matching to parton shower simulations", *JHEP* **07** (2014) 079, doi:10.1007/JHEP07(2014)079, arXiv:1405.0301.

[57] NNPDF Collaboration, "Parton distributions for the LHC Run II", *JHEP* **04** (2015) 040, doi:10.1007/JHEP04(2015)040, arXiv:1410.8849.

[58] NNPDF Collaboration, "Parton distributions from high-precision collider data", *Eur. Phys. J. C* **77** (2017) 663, doi:10.1140/epjc/s10052-017-5199-5, arXiv:1706.00428.

[59] B. Fuks, M. Klasen, D. R. Lamprea, and M. Rothering, "Revisiting slepton pair production at the Large Hadron Collider", *JHEP* **01** (2014) 168, doi:10.1007/JHEP01(2014)168, arXiv:1310.2621.

[60] B. Fuks, M. Klasen, D. R. Lamprea, and M. Rothering, "Precision predictions for electroweak superpartner production at hadron colliders with Resummino", *Eur. Phys. J. C* **73** (2013) 2480, doi:10.1140/epjc/s10052-013-2480-0, arXiv:1304.0790.

[61] J. Fiaschi, B. Fuks, M. Klasen, and A. Neuwirth, "Electroweak superpartner production at 13.6 Tev with Resummino", *Eur. Phys. J. C* **83** (2023) 707, doi:10.1140/epjc/s10052-023-11888-y, arXiv:2304.11915.

[62] J. Fiaschi and M. Klasen, "Slepton pair production at the LHC in NLO+NLL with resummation-improved parton densities", *JHEP* **03** (2018) 094, doi:10.1007/JHEP03(2018)094, arXiv:1801.10357.

[63] G. Bozzi, B. Fuks, and M. Klasen, "Joint resummation for slepton pair production at hadron colliders", *Nucl. Phys. B* **794** (2008) 46, doi:10.1016/j.nuclphysb.2007.10.021, arXiv:0709.3057.

[64] G. Bozzi, B. Fuks, and M. Klasen, "Transverse-momentum resummation for slepton-pair production at the CERN LHC", *Phys. Rev. D* **74** (2006) 015001, doi:10.1103/PhysRevD.74.015001, arXiv:hep-ph/0603074.

[65] A. P. Neuwirth, "HEPi", 2024. doi:10.5281/zenodo.8430836.

[66] C. Oleari, "The POWHEG-BOX", *Nucl. Phys. B Proc. Suppl.* **205-206** (2010) 36, doi:10.1016/j.nuclphysbps.2010.08.016, arXiv:1007.3893.

[67] P. Nason, "A new method for combining NLO QCD with shower Monte Carlo algorithms", *JHEP* **11** (2004) 040, doi:10.1088/1126-6708/2004/11/040, arXiv:hep-ph/0409146.

[68] S. Frixione, P. Nason, and C. Oleari, "Matching NLO QCD computations with parton shower simulations: the POWHEG method", *JHEP* **11** (2007) 070, doi:10.1088/1126-6708/2007/11/070, arXiv:0709.2092.

[69] S. Alioli, P. Nason, C. Oleari, and E. Re, "A general framework for implementing NLO calculations in shower Monte Carlo programs: the POWHEG BOX", *JHEP* **06** (2010) 043, doi:10.1007/JHEP06(2010)043, arXiv:1002.2581.

[70] S. Frixione, P. Nason, and G. Ridolfi, "A positive-weight next-to-leading-order Monte Carlo for heavy flavour hadroproduction", *JHEP* **09** (2007) 126, doi:10.1088/1126-6708/2007/09/126, arXiv:0707.3088.

[71] GEANT4 Collaboration, "GEANT4 – a simulation toolkit", *Nucl. Instrum. Meth. A* **506** (2003) 250, doi:10.1016/S0168-9002(03)01368-8.

[72] T. Sjöstrand et al., "An introduction to PYTHIA 8.2", *Comput. Phys. Commun.* **191** (2015) 159, doi:10.1016/j.cpc.2015.01.024, arXiv:1410.3012.

[73] CMS Collaboration, "Extraction and validation of a new set of CMS PYTHIA8 tunes from underlying-event measurements", *Eur. Phys. J. C* **80** (2020) 4, doi:10.1140/epjc/s10052-019-7499-4, arXiv:1903.12179.

[74] CMS Collaboration, "Particle-flow reconstruction and global event description with the CMS detector", *JINST* **12** (2017) P10003, doi:10.1088/1748-0221/12/10/P10003, arXiv:1706.04965.

[75] CMS Collaboration, "Technical proposal for the Phase-II upgrade of the Compact Muon Solenoid", CMS Technical proposal CERN-LHCC-2015-010, CMS-TDR-15-02, 2015.

[76] M. Cacciari, G. P. Salam, and G. Soyez, "The anti-k_{T} jet clustering algorithm", *JHEP* **04** (2008) 063, doi:10.1088/1126-6708/2008/04/063, arXiv:0802.1189.

[77] M. Cacciari, G. P. Salam, and G. Soyez, "FastJet user manual", *Eur. Phys. J. C* **72** (2012) 1896, doi:10.1140/epjc/s10052-012-1896-2, arXiv:1111.6097.

[78] CMS Collaboration, "Jet energy scale and resolution in the CMS experiment in pp collisions at 8 TeV", *JINST* **12** (2017) P02014, doi:10.1088/1748-0221/12/02/P02014, arXiv:1607.03663.

[79] CMS Collaboration, "Jet algorithms performance in 13 TeV data", CMS Physics Analysis Summary CMS-PAS-JME-16-003, 2017.

[80] CMS Collaboration, "Track impact parameter resolution for the full pseudo rapidity coverage in the 2017 dataset with the CMS Phase-1 pixel detector", CMS Detector Performance Summary CMS-DP-2020-049, 2020.

[81] CMS Collaboration, "Description and performance of track and primary-vertex reconstruction with the CMS tracker", *JINST* **9** (2014) P10009, doi:10.1088/1748-0221/9/10/P10009, arXiv:1405.6569.

[82] CMS Collaboration, "Identification of heavy-flavour jets with the CMS detector in pp collisions at 13 TeV", *JINST* **13** (2018) P05011, doi:10.1088/1748-0221/13/05/P05011, arXiv:1712.07158.

[83] CMS Collaboration, "Performance summary of AK4 jet b tagging with data from proton-proton collisions at 13 TeV with the CMS detector", CMS Detector Performance Note CMS-DP-2023-005, 2023.

[84] E. Bols et al., "Jet flavour classification using DEEPJET", *JINST* **15** (2020) P12012, doi:10.1088/1748-0221/15/12/P12012, arXiv:2008.10519.

[85] CMS Collaboration, "Electron and photon reconstruction and identification with the CMS experiment at the CERN LHC", *JINST* **16** (2021) P05014, doi:10.1088/1748-0221/16/05/P05014, arXiv:2012.06888.

[86] CMS Collaboration, "Performance of electron reconstruction and selection with the CMS detector in proton-proton collisions at $\sqrt{s} = 8$ TeV", *JINST* **10** (2015) P06005, doi:10.1088/1748-0221/10/06/P06005, arXiv:1502.02701.

[87] CMS Collaboration, "Performance of the CMS muon detector and muon reconstruction with proton-proton collisions at $\sqrt{s} = 13$ TeV", *JINST* **13** (2018) P06015, doi:10.1088/1748-0221/13/06/P06015, arXiv:1804.04528.

[88] CMS Collaboration, "Pileup mitigation at CMS in 13 TeV data", *JINST* **15** (2020) P09018, doi:10.1088/1748-0221/15/09/P09018, arXiv:2003.00503.

[89] CMS Collaboration, "Performance of missing transverse momentum reconstruction in proton-proton collisions at $\sqrt{s} = 13$ TeV using the CMS detector", *JINST* **14** (2019) P07004, doi:10.1088/1748-0221/14/07/P07004, arXiv:1903.06078.

[90] Y. Wang et al., "Dynamic graph CNN for learning on point clouds", *ACM Trans. Graph.* **38** (2019) doi:10.1145/3326362.

[91] CMS Collaboration, "Observation of the Higgs boson decay to a pair of τ leptons with the CMS detector", *Phys. Lett. B* **779** (2018) 283, doi:10.1016/j.physletb.2018.02.004, arXiv:1708.00373.

[92] CMS Collaboration, "Search for neutral MSSM Higgs bosons decaying to a pair of tau leptons in pp collisions", *JHEP* **10** (2014) 160, doi:10.1007/JHEP10(2014)160, arXiv:1408.3316.

[93] CMS Collaboration, "Measurements of Inclusive W and Z Cross Sections in pp Collisions at $\sqrt{s} = 7$ TeV", *JHEP* **01** (2011) 080, doi:10.1007/JHEP01(2011)080, arXiv:1012.2466.

[94] C. G. Lester and D. J. Summers, "Measuring masses of semiinvisibly decaying particles pair produced at hadron colliders", *Phys. Lett. B* **463** (1999) 99, doi:10.1016/S0370-2693(99)00945-4, arXiv:hep-ph/9906349.

[95] A. Barr, C. Lester, and P. Stephens, "m_{T2}: The truth behind the glamour", *J. Phys. G* **29** (2003) 2343, doi:10.1088/0954-3899/29/10/304, arXiv:hep-ph/0304226.

[96] A. J. Barr and C. Gwenlan, "The race for supersymmetry: Using m_{T2} for discovery", *Phys. Rev. D* **80** (2009) 074007, doi:10.1103/PhysRevD.80.074007, arXiv:0907.2713.

[97] CMS Collaboration, "Search for long-lived particles using out-of-time trackless jets in proton-proton collisions at $\sqrt{s}$ = 13 TeV", *JHEP* **07** (2023) 210, doi:10.1007/JHEP07(2023)210, arXiv:2212.06695.

[98] CMS Collaboration, "Search for top squark pair production in a final state with at least one hadronically decaying tau lepton in proton-proton collisions at $\sqrt{s}$ = 13 TeV", *JHEP* **07** (2023) 110, doi:10.1007/JHEP07(2023)110, arXiv:2304.07174.

[99] J. Butterworth et al., "PDF4LHC recommendations for LHC Run II", *J. Phys. G* **43** (2016) 023001, doi:10.1088/0954-3899/43/2/023001, arXiv:1510.03865.

[100] A. Kalogeropoulos and J. Alwall, "The SysCalc code: A tool to derive theoretical systematic uncertainties", 2018. arXiv:1801.08401.

[101] CMS Collaboration, "Measurement of the inelastic proton-proton cross section at $\sqrt{s} = 13$ TeV", *JHEP* **07** (2018) 161, doi:10.1007/JHEP07(2018)161, arXiv:1802.02613.

[102] CMS Collaboration, "Precision luminosity measurement in proton-proton collisions at $\sqrt{s} = 13$ TeV in 2015 and 2016 at CMS", *Eur. Phys. J. C* **81** (2021) 800, doi:10.1140/epjc/s10052-021-09538-2, arXiv:2104.01927.

[103] CMS Collaboration, "CMS luminosity measurement for the 2017 data-taking period at $\sqrt{s} = 13$ TeV", CMS Physics Analysis Summary CMS-PAS-LUM-17-004, 2018.

[104] CMS Collaboration, "CMS luminosity measurement for the 2018 data-taking period at $\sqrt{s} = 13$ TeV", CMS Physics Analysis Summary CMS-PAS-LUM-18-002, 2019.

[105] CMS Collaboration, "Operation and performance of the CMS silicon strip tracker with proton-proton collisions at the CERN LHC", *JINST* **20** (2025) P08027, doi:10.1088/1748-0221/20/08/P08027, arXiv:2506.17195.

[106] ATLAS and CMS Collaborations, and the LHC Higgs Combination Group, "Procedure for the LHC Higgs boson search combination in summer 2011", Technical Report CMS-NOTE-2011-005, ATL-PHYS-PUB-2011-11, 2011.

[107] T. Junk, "Confidence level computation for combining searches with small statistics", *Nucl. Instrum. Meth. A* **434** (1999) 435, doi:10.1016/S0168-9002(99)00498-2, arXiv:hep-ex/9902006.

[108] A. L. Read, "Presentation of search results: the CL_s technique", *J. Phys. G* **28** (2002) 2693, doi:10.1088/0954-3899/28/10/313.

[109] CMS Collaboration, "The CMS statistical analysis and combination tool: Combine", *Comput. Softw. Big Sci.* **8** (2024) 19, doi:10.1007/s41781-024-00121-4, arXiv:2404.06614.

A The CMS Collaboration

Yerevan Physics Institute, Yerevan, Armenia
A. Hayrapetyan, V. Makarenko, A. Tumasyan[1]

Institut für Hochenergiephysik, Vienna, Austria
W. Adam, L. Benato, T. Bergauer, M. Dragicevic, P.S. Hussain, M. Jeitler[2], N. Krammer, A. Li, D. Liko, M. Matthewman, J. Schieck[2], R. Schöfbeck[2], M. Shooshtari, M. Sonawane, W. Waltenberger, C.-E. Wulz[2]

Universiteit Antwerpen, Antwerpen, Belgium
T. Janssen, H. Kwon, D. Ocampo Henao, T. Van Laer, P. Van Mechelen

Vrije Universiteit Brussel, Brussel, Belgium
J. Bierkens, N. Breugelmans, J. D'Hondt, S. Dansana, A. De Moor, M. Delcourt, F. Heyen, Y. Hong, P. Kashko, S. Lowette, I. Makarenko, D. Müller, S. Tavernier, M. Tytgat[3], G.P. Van Onsem, S. Van Putte, D. Vannerom

Université Libre de Bruxelles, Bruxelles, Belgium
B. Bilin, B. Clerbaux, A.K. Das, I. De Bruyn, G. De Lentdecker, H. Evard, L. Favart, P. Gianneios, A. Khalilzadeh, F.A. Khan, A. Malara, M.A. Shahzad, A. Sharma, L. Thomas, M. Vanden Bemden, C. Vander Velde, P. Vanlaer, F. Zhang

Ghent University, Ghent, Belgium
M. De Coen, D. Dobur, C. Giordano, G. Gokbulut, K. Kaspar, D. Kavtaradze, D. Marckx, K. Skovpen, A.M. Tomaru, N. Van Den Bossche, J. van der Linden, J. Vandenbroeck

Université Catholique de Louvain, Louvain-la-Neuve, Belgium
H. Aarup Petersen, S. Bein, A. Benecke, A. Bethani, G. Bruno, A. Cappati, J. De Favereau De Jeneret, C. Delaere, F. Gameiro Casalinho, A. Giammanco, A.O. Guzel, V. Lemaitre, J. Lidrych, P. Malek, P. Mastrapasqua, S. Turkcapar

Centro Brasileiro de Pesquisas Fisicas, Rio de Janeiro, Brazil
G.A. Alves, M. Barroso Ferreira Filho, E. Coelho, C. Hensel, D. Matos Figueiredo, T. Menezes De Oliveira, C. Mora Herrera, P. Rebello Teles, M. Soeiro, E.J. Tonelli Manganote[4], A. Vilela Pereira

Universidade do Estado do Rio de Janeiro, Rio de Janeiro, Brazil
W.L. Aldá Júnior, H. Brandao Malbouisson, W. Carvalho, J. Chinellato[5], M. Costa Reis, E.M. Da Costa, G.G. Da Silveira[6], D. De Jesus Damiao, S. Fonseca De Souza, R. Gomes De Souza, S. S. Jesus, T. Laux Kuhn[6], M. Macedo, K. Mota Amarilo, L. Mundim, H. Nogima, J.P. Pinheiro, A. Santoro, A. Sznajder, M. Thiel, F. Torres Da Silva De Araujo[7]

Universidade Estadual Paulista, Universidade Federal do ABC, São Paulo, Brazil
C.A. Bernardes[6], L. Calligaris, F. Damas, T.R. Fernandez Perez Tomei, E.M. Gregores, B. Lopes Da Costa, I. Maietto Silverio, P.G. Mercadante, S.F. Novaes, Sandra S. Padula, V. Scheurer

Institute for Nuclear Research and Nuclear Energy, Bulgarian Academy of Sciences, Sofia, Bulgaria
A. Aleksandrov, G. Antchev, P. Danev, R. Hadjiiska, P. Iaydjiev, M. Shopova, G. Sultanov

University of Sofia, Sofia, Bulgaria
A. Dimitrov, L. Litov, B. Pavlov, P. Petkov, A. Petrov

Instituto De Alta Investigación, Universidad de Tarapacá, Casilla 7 D, Arica, Chile
S. Keshri, D. Laroze, S. Thakur

Universidad Tecnica Federico Santa Maria, Valparaiso, Chile
W. Brooks

Beihang University, Beijing, China
T. Cheng, T. Javaid, L. Wang, L. Yuan

Department of Physics, Tsinghua University, Beijing, China
Z. Hu, Z. Liang, J. Liu, X. Wang, H. Yang

Institute of High Energy Physics, Beijing, China
G.M. Chen[8], H.S. Chen[8], M. Chen[8], Y. Chen, Q. Hou, X. Hou, F. Iemmi, C.H. Jiang, H. Liao, G. Liu, Z.-A. Liu[9], J.N. Song[9], S. Song, J. Tao, C. Wang[8], J. Wang, H. Zhang, J. Zhao

State Key Laboratory of Nuclear Physics and Technology, Peking University, Beijing, China
A. Agapitos, Y. Ban, A. Carvalho Antunes De Oliveira, S. Deng, B. Guo, Q. Guo, C. Jiang, A. Levin, C. Li, Q. Li, Y. Mao, S. Qian, S.J. Qian, X. Qin, C. Quaranta, X. Sun, D. Wang, J. Wang, M. Zhang, Y. Zhao, C. Zhou

State Key Laboratory of Nuclear Physics and Technology, Institute of Quantum Matter, South China Normal University, Guangzhou, China
S. Yang

Sun Yat-Sen University, Guangzhou, China
Z. You

University of Science and Technology of China, Hefei, China
K. Jaffel, N. Lu

Nanjing Normal University, Nanjing, China
G. Bauer[10,11], Z. Cui[11], B. Li[12], H. Wang, K. Yi[13], J. Zhang

Institute of Modern Physics and Key Laboratory of Nuclear Physics and Ion-beam Application (MOE) - Fudan University, Shanghai, China
Y. Li, Y. Zhou[14]

Zhejiang University, Hangzhou, Zhejiang, China
Z. Lin, C. Lu, M. Xiao[15]

Universidad de Los Andes, Bogota, Colombia
C. Avila, D.A. Barbosa Trujillo, A. Cabrera, C. Florez, J. Fraga, J.A. Reyes Vega

Universidad de Antioquia, Medellin, Colombia
C. Rendón, M. Rodriguez, A.A. Ruales Barbosa, J.D. Ruiz Alvarez

University of Split, Faculty of Electrical Engineering, Mechanical Engineering and Naval Architecture, Split, Croatia
N. Godinovic, D. Lelas, A. Sculac

University of Split, Faculty of Science, Split, Croatia
M. Kovac, A. Petkovic, T. Sculac

Institute Rudjer Boskovic, Zagreb, Croatia
P. Bargassa, V. Brigljevic, B.K. Chitroda, D. Ferencek, K. Jakovcic, A. Starodumov, T. Susa

University of Cyprus, Nicosia, Cyprus
A. Attikis, K. Christoforou, S. Konstantinou, C. Leonidou, L. Paizanos, F. Ptochos, P.A. Razis, H. Rykaczewski, H. Saka, A. Stepennov

Charles University, Prague, Czech Republic
M. Finger[†], M. Finger Jr.

Escuela Politecnica Nacional, Quito, Ecuador
E. Ayala

Universidad San Francisco de Quito, Quito, Ecuador
E. Carrera Jarrin

Academy of Scientific Research and Technology of the Arab Republic of Egypt, Egyptian Network of High Energy Physics, Cairo, Egypt
H. Abdalla[16], Y. Assran[17,18]

Center for High Energy Physics (CHEP-FU), Fayoum University, El-Fayoum, Egypt
A. Hussein, H. Mohammed

National Institute of Chemical Physics and Biophysics, Tallinn, Estonia
M. Kadastik, T. Lange, C. Nielsen, J. Pata, M. Raidal, N. Seeba, L. Tani

Department of Physics, University of Helsinki, Helsinki, Finland
E. Brücken, A. Milieva, K. Osterberg, M. Voutilainen

Helsinki Institute of Physics, Helsinki, Finland
F. Garcia, P. Inkaew, K.T.S. Kallonen, R. Kumar Verma, T. Lampén, K. Lassila-Perini, B. Lehtela, S. Lehti, T. Lindén, N.R. Mancilla Xinto, M. Myllymäki, M.m. Rantanen, S. Saariokari, N.T. Toikka, J. Tuominiemi

Lappeenranta-Lahti University of Technology, Lappeenranta, Finland
N. Bin Norjoharuddeen, H. Kirschenmann, P. Luukka, H. Petrow

IRFU, CEA, Université Paris-Saclay, Gif-sur-Yvette, France
M. Besancon, F. Couderc, M. Dejardin, D. Denegri, P. Devouge, J.L. Faure, F. Ferri, P. Gaigne, S. Ganjour, P. Gras, F. Guilloux, G. Hamel de Monchenault, M. Kumar, V. Lohezic, Y. Maidannyk, J. Malcles, F. Orlandi, L. Portales, S. Ronchi, M.Ö. Sahin, A. Savoy-Navarro[19], P. Simkina, M. Titov, M. Tornago

Laboratoire Leprince-Ringuet, CNRS/IN2P3, Ecole Polytechnique, Institut Polytechnique de Paris, Palaiseau, France
R. Amella Ranz, F. Beaudette, G. Boldrini, P. Busson, C. Charlot, M. Chiusi, T.D. Cuisset, O. Davignon, A. De Wit, T. Debnath, I.T. Ehle, S. Ghosh, A. Gilbert, R. Granier de Cassagnac, L. Kalipoliti, M. Manoni, M. Nguyen, S. Obraztsov, C. Ochando, R. Salerno, J.B. Sauvan, Y. Sirois, G. Sokmen, L. Urda Gómez, A. Zabi, A. Zghiche

Université de Strasbourg, CNRS, IPHC UMR 7178, Strasbourg, France
J.-L. Agram[20], J. Andrea, D. Bloch, J.-M. Brom, E.C. Chabert, C. Collard, G. Coulon, S. Falke, U. Goerlach, R. Haeberle, A.-C. Le Bihan, M. Meena, O. Poncet, G. Saha, P. Vaucelle

Centre de Calcul de l'Institut National de Physique Nucleaire et de Physique des Particules, CNRS/IN2P3, Villeurbanne, France
A. Di Florio, B. Orzari

Institut de Physique des 2 Infinis de Lyon (IP2I), Villeurbanne, France
D. Amram, S. Beauceron, B. Blancon, G. Boudoul, N. Chanon, D. Contardo, P. Depasse, H. El Mamouni, J. Fay, E. Fillaudeau, S. Gascon, M. Gouzevitch, C. Greenberg, G. Grenier, B. Ille, E. Jourd'Huy, M. Lethuillier, B. Massoteau, L. Mirabito, A. Purohit, M. Vander Donckt, J. Xiao

Georgian Technical University, Tbilisi, Georgia
G. Adamov, I. Lomidze, Z. Tsamalaidze[21]

RWTH Aachen University, I. Physikalisches Institut, Aachen, Germany
V. Botta, S. Consuegra Rodríguez, L. Feld, K. Klein, M. Lipinski, P. Nattland, V. Oppenländer, A. Pauls, D. Pérez Adán, N. Röwert

RWTH Aachen University, III. Physikalisches Institut A, Aachen, Germany
C. Daumann, S. Diekmann, N. Eich, D. Eliseev, F. Engelke, J. Erdmann, M. Erdmann, B. Fischer, T. Hebbeker, K. Hoepfner, F. Ivone, A. Jung, N. Kumar, M.y. Lee, F. Mausolf, M. Merschmeyer, A. Meyer, A. Pozdnyakov, W. Redjeb, H. Reithler, U. Sarkar, V. Sarkisovi, A. Schmidt, C. Seth, A. Sharma, J.L. Spah, V. Vaulin, S. Zaleski

RWTH Aachen University, III. Physikalisches Institut B, Aachen, Germany
M.R. Beckers, C. Dziwok, G. Flügge, N. Hoeflich, T. Kress, A. Nowack, O. Pooth, A. Stahl, A. Zotz

Deutsches Elektronen-Synchrotron, Hamburg, Germany
A. Abel, M. Aldaya Martin, J. Alimena, S. Amoroso, Y. An, I. Andreev, J. Bach, S. Baxter, H. Becerril Gonzalez, O. Behnke, A. Belvedere, F. Blekman[22], K. Borras[23], A. Campbell, S. Chatterjee, L.X. Coll Saravia, G. Eckerlin, D. Eckstein, E. Gallo[22], A. Geiser, M. Guthoff, A. Hinzmann, L. Jeppe, M. Kasemann, C. Kleinwort, R. Kogler, M. Komm, D. Krücker, W. Lange, D. Leyva Pernia, K.-Y. Lin, K. Lipka[24], W. Lohmann[25], J. Malvaso, R. Mankel, I.-A. Melzer-Pellmann, M. Mendizabal Morentin, A.B. Meyer, G. Milella, K. Moral Figueroa, A. Mussgiller, L.P. Nair, J. Niedziela, A. Nürnberg, J. Park, E. Ranken, A. Raspereza, D. Rastorguev, L. Rygaard, M. Scham[26,23], S. Schnake[23], P. Schütze, C. Schwanenberger[22], D. Schwarz, D. Selivanova, K. Sharko, M. Shchedrolosiev, D. Stafford, M. Torkian, A. Ventura Barroso, R. Walsh, D. Wang, Q. Wang, K. Wichmann, L. Wiens[23], C. Wissing, Y. Yang, S. Zakharov, A. Zimermmane Castro Santos

University of Hamburg, Hamburg, Germany
A.R. Alves Andrade, M. Antonello, S. Bollweg, M. Bonanomi, L. Ebeling, K. El Morabit, Y. Fischer, M. Frahm, E. Garutti, A. Grohsjean, A.A. Guvenli, J. Haller, D. Hundhausen, G. Kasieczka, P. Keicher, R. Klanner, W. Korcari, T. Kramer, C.c. Kuo, F. Labe, J. Lange, A. Lobanov, J. Matthiesen, L. Moureaux, K. Nikolopoulos, A. Paasch, K.J. Pena Rodriguez, N. Prouvost, B. Raciti, M. Rieger, D. Savoiu, P. Schleper, M. Schröder, J. Schwandt, M. Sommerhalder, H. Stadie, G. Steinbrück, R. Ward, B. Wiederspan, M. Wolf, C. Yede

Karlsruher Institut fuer Technologie, Karlsruhe, Germany

S. Brommer, A. Brusamolino, E. Butz, Y.M. Chen, T. Chwalek, A. Dierlamm, G.G. Dincer, D. Druzhkin, U. Elicabuk, N. Faltermann, M. Giffels, A. Gottmann, F. Hartmann[27], M. Horzela, F. Hummer, U. Husemann, J. Kieseler, M. Klute, J. Knolle, R. Kunnilan Muhammed Rafeek, O. Lavoryk, J.M. Lawhorn, S. Maier, A.A. Monsch, M. Mormile, Th. Müller, E. Pfeffer, M. Presilla, G. Quast, K. Rabbertz, B. Regnery, R. Schmieder, N. Shadskiy, I. Shvetsov, H.J. Simonis, L. Sowa, L. Stockmeier, K. Tauqeer, M. Toms, B. Topko, N. Trevisani, C. Verstege, T. Voigtländer, R.F. Von Cube, J. Von Den Driesch, C. Winter, R. Wolf, W.D. Zeuner, X. Zuo

Institute of Nuclear and Particle Physics (INPP), NCSR Demokritos, Aghia Paraskevi, Greece
G. Anagnostou, G. Daskalakis, A. Kyriakis

National and Kapodistrian University of Athens, Athens, Greece
G. Melachroinos, Z. Painesis, I. Paraskevas, N. Saoulidou, K. Theofilatos, E. Tziaferi, E. Tzovara, K. Vellidis, I. Zisopoulos

National Technical University of Athens, Athens, Greece
T. Chatzistavrou, G. Karapostoli, K. Kousouris, E. Siamarkou, G. Tsipolitis

University of Ioánnina, Ioánnina, Greece
I. Bestintzanos, I. Evangelou, C. Foudas, P. Katsoulis, P. Kokkas, P.G. Kosmoglou Kioseoglou, N. Manthos, I. Papadopoulos, J. Strologas

HUN-REN Wigner Research Centre for Physics, Budapest, Hungary
C. Hajdu, D. Horvath[28,29], Á. Kadlecsik, K. Márton, A.J. Rádl[30], F. Sikler, V. Veszpremi

MTA-ELTE Lendület CMS Particle and Nuclear Physics Group, Eötvös Loránd University, Budapest, Hungary
M. Csanád, K. Farkas, A. Fehérkuti[31], M.M.A. Gadallah[32], M. León Coello, G. Pásztor, G.I. Veres

Faculty of Informatics, University of Debrecen, Debrecen, Hungary
B. Ujvari, G. Zilizi

HUN-REN ATOMKI - Institute of Nuclear Research, Debrecen, Hungary
G. Bencze, S. Czellar, J. Molnar, Z. Szillasi

Karoly Robert Campus, MATE Institute of Technology, Gyongyos, Hungary
T. Csorgo[31], F. Nemes[31], T. Novak, I. Szanyi[33]

IIT Bhubaneswar, Bhubaneswar, India
S. Bahinipati, S. Nayak, R. Raturi

Panjab University, Chandigarh, India
S. Bansal, S.B. Beri, V. Bhatnagar, S. Chauhan, N. Dhingra[34], A. Kaur, H. Kaur, M. Kaur, S. Kumar, T. Sheokand, J.B. Singh, A. Singla

University of Delhi, Delhi, India
A. Bhardwaj, A. Chhetri, B.C. Choudhary, A. Kumar, A. Kumar, M. Naimuddin, S. Phor, K. Ranjan, M.K. Saini

Indian Institute of Technology Mandi (IIT-Mandi), Himachal Pradesh, India
P. Palni

University of Hyderabad, Hyderabad, India
S. Acharya[35], B. Gomber

Indian Institute of Technology Kanpur, Kanpur, India
S. Mukherjee

Saha Institute of Nuclear Physics, HBNI, Kolkata, India
S. Bhattacharya, S. Das Gupta, S. Dutta, S. Dutta, S. Sarkar

Indian Institute of Technology Madras, Madras, India
M.M. Ameen, P.K. Behera, S. Chatterjee, G. Dash, A. Dattamunsi, P. Jana, P. Kalbhor, S. Kamble, J.R. Komaragiri[36], T. Mishra, P.R. Pujahari, A.K. Sikdar, R.K. Singh, P. Verma, S. Verma, A. Vijay

IISER Mohali, India, Mohali, India
B.K. Sirasva

Tata Institute of Fundamental Research-A, Mumbai, India
L. Bhatt, S. Dugad, G.B. Mohanty, M. Shelake, P. Suryadevara

Tata Institute of Fundamental Research-B, Mumbai, India
A. Bala, S. Banerjee, S. Barman[37], R.M. Chatterjee, M. Guchait, Sh. Jain, A. Jaiswal, S. Kumar, M. Maity[37], G. Majumder, K. Mazumdar, S. Parolia, R. Saxena, A. Thachayath

National Institute of Science Education and Research, An OCC of Homi Bhabha National Institute, Bhubaneswar, Odisha, India
D. Maity[38], P. Mal, K. Naskar[38], A. Nayak[38], K. Pal, P. Sadangi, S.K. Swain, S. Varghese[38], D. Vats[38]

Indian Institute of Science Education and Research (IISER), Pune, India
S. Dube, P. Hazarika, B. Kansal, A. Laha, R. Sharma, S. Sharma, K.Y. Vaish

Indian Institute of Technology Hyderabad, Telangana, India
S. Ghosh

Isfahan University of Technology, Isfahan, Iran
H. Bakhshiansohi[39], A. Jafari[40], V. Sedighzadeh Dalavi, M. Zeinali[41]

Institute for Research in Fundamental Sciences (IPM), Tehran, Iran
S. Bashiri, S. Chenarani[42], S.M. Etesami, Y. Hosseini, M. Khakzad, E. Khazaie, M. Mohammadi Najafabadi, S. Tizchang[43]

University College Dublin, Dublin, Ireland
M. Felcini, M. Grunewald

INFN Sezione di Bari[a], Università di Bari[b], Politecnico di Bari[c], Bari, Italy
M. Abbrescia[a,b], M. Barbieri[a,b], M. Buonsante[a,b], A. Colaleo[a,b], D. Creanza[a,c], N. De Filippis[a,c], M. De Palma[a,b], W. Elmetenawee[a,b,44], N. Ferrara[a,c], L. Fiore[a], L. Generoso[a,b], L. Longo[a], M. Louka[a,b], G. Maggi[a,c], M. Maggi[a], I. Margjeka[a], V. Mastrapasqua[a,b], S. My[a,b], F. Nenna[a,b], S. Nuzzo[a,b], A. Pellecchia[a,b], A. Pompili[a,b], G. Pugliese[a,c], R. Radogna[a,b], D. Ramos[a], A. Ranieri[a], L. Silvestris[a], F.M. Simone[a,c], Ü. Sözbilir[a], A. Stamerra[a,b], D. Troiano[a,b], R. Venditti[a,b], P. Verwilligen[a], A. Zaza[a,b]

INFN Sezione di Bologna[a], Università di Bologna[b], Bologna, Italy

G. Abbiendi[a], C. Battilana[a,b], D. Bonacorsi[a,b], P. Capiluppi[a,b], F.R. Cavallo[a], M. Cuffiani[a,b], G.M. Dallavalle[a], T. Diotalevi[a,b], F. Fabbri[a], A. Fanfani[a,b], R. Farinelli[a], P. Giacomelli[a], C. Grandi[a], L. Guiducci[a,b], S. Lo Meo[a,45], M. Lorusso[a,b], L. Lunerti[a], S. Marcellini[a], F.L. Navarria[a,b], G. Paggi[a,b], A. Perrotta[a], A.M. Rossi[a,b], S. Rossi Tisbeni[a,b], T. Rovelli[a,b], G.P. Siroli[a,b]

INFN Sezione di Catania[a], Università di Catania[b], Catania, Italy
S. Costa[a,b,46], A. Di Mattia[a], A. Lapertosa[a], R. Potenza[a,b], A. Tricomi[a,b,46]

INFN Sezione di Firenze[a], Università di Firenze[b], Firenze, Italy
J. Altork[a,b], P. Assiouras[a], G. Barbagli[a], G. Bardelli[a], M. Bartolini[a,b], A. Calandri[a,b], B. Camaiani[a,b], A. Cassese[a], R. Ceccarelli[a], V. Ciulli[a,b], C. Civinini[a], R. D'Alessandro[a,b], L. Damenti[a,b], E. Focardi[a,b], T. Kello[a], G. Latino[a,b], P. Lenzi[a,b], M. Lizzo[a], M. Meschini[a], S. Paoletti[a], A. Papanastassiou[a,b], G. Sguazzoni[a], L. Viliani[a]

INFN Laboratori Nazionali di Frascati, Frascati, Italy
L. Benussi, S. Bianco, S. Meola[47], D. Piccolo

INFN Sezione di Genova[a], Università di Genova[b], Genova, Italy
M. Alves Gallo Pereira[a], F. Ferro[a], E. Robutti[a], S. Tosi[a,b]

INFN Sezione di Milano-Bicocca[a], Università di Milano-Bicocca[b], Milano, Italy
A. Benaglia[a], F. Brivio[a], V. Camagni[a,b], F. Cetorelli[a,b], F. De Guio[a,b], M.E. Dinardo[a,b], P. Dini[a], S. Gennai[a], R. Gerosa[a,b], A. Ghezzi[a,b], P. Govoni[a,b], L. Guzzi[a], M.R. Kim[a], G. Lavizzari[a,b], M.T. Lucchini[a,b], M. Malberti[a], S. Malvezzi[a], A. Massironi[a], D. Menasce[a], L. Moroni[a], M. Paganoni[a,b], S. Palluotto[a,b], D. Pedrini[a], A. Perego[a,b], G. Pizzati[a,b], T. Tabarelli de Fatis[a,b]

INFN Sezione di Napoli[a], Università di Napoli 'Federico II'[b], Napoli, Italy; Università della Basilicata[c], Potenza, Italy; Scuola Superiore Meridionale (SSM)[d], Napoli, Italy
S. Buontempo[a], C. Di Fraia[a,b], F. Fabozzi[a,c], L. Favilla[a,d], A.O.M. Iorio[a,b], L. Lista[a,b,48], P. Paolucci[a,27], B. Rossi[a]

INFN Sezione di Padova[a], Università di Padova[b], Padova, Italy; Universita degli Studi di Cagliari[c], Cagliari, Italy
P. Azzi[a], N. Bacchetta[a,49], D. Bisello[a,b], L. Borella[a], P. Bortignon[a,c], G. Bortolato[a,b], A.C.M. Bulla[a,c], R. Carlin[a,b], P. Checchia[a], T. Dorigo[a,50], U. Gasparini[a,b], S. Giorgetti[a], E. Lusiani[a], M. Margoni[a,b], A.T. Meneguzzo[a,b], J. Pazzini[a,b], F. Primavera[a,b], P. Ronchese[a,b], R. Rossin[a,b], M. Sgaravatto[a], F. Simonetto[a,b], M. Tosi[a,b], A. Triossi[a,b], M. Zanetti[a,b], P. Zotto[a,b], A. Zucchetta[a,b], G. Zumerle[a,b]

INFN Sezione di Pavia[a], Università di Pavia[b], Pavia, Italy
A. Braghieri[a], M. Brunoldi[a,b], S. Calzaferri[a,b], P. Montagna[a,b], M. Pelliccioni[a,b], V. Re[a], C. Riccardi[a,b], P. Salvini[a], I. Vai[a,b], P. Vitulo[a,b]

INFN Sezione di Perugia[a], Università di Perugia[b], Perugia, Italy
S. Ajmal[a,b], M.E. Ascioti[a,b], G.M. Bilei[†a], C. Carrivale[a,b], D. Ciangottini[a,b], L. Della Penna[a,b], L. Fanò[a,b], V. Mariani[a,b], M. Menichelli[a], F. Moscatelli[a,51], A. Rossi[a,b], A. Santocchia[a,b], D. Spiga[a], T. Tedeschi[a,b]

INFN Sezione di Pisa[a], Università di Pisa[b], Scuola Normale Superiore di Pisa[c], Pisa, Italy; Università di Siena[d], Siena, Italy

C. Aimè[a,b], C.A. Alexe[a,c], P. Asenov[a,b], P. Azzurri[a], G. Bagliesi[a], L. Bianchini[a,b], T. Boccali[a], E. Bossini[a], D. Bruschini[a,c], R. Castaldi[a], F. Cattafesta[a,c], M.A. Ciocci[a,d], M. Cipriani[a,b], R. Dell'Orso[a], S. Donato[a,b], R. Forti[a,b], A. Giassi[a], F. Ligabue[a,c], A.C. Marini[a,b], A. Messineo[a,b], S. Mishra[a], V.K. Muraleedharan Nair Bindhu[a,b], S. Nandan[a], F. Palla[a], M. Riggirello[a,c], A. Rizzi[a,b], G. Rolandi[a,c], S. Roy Chowdhury[a,52], T. Sarkar[a], A. Scribano[a], P. Solanki[a,b], P. Spagnolo[a], F. Tenchini[a,b], R. Tenchini[a], G. Tonelli[a,b], N. Turini[a,d], F. Vaselli[a,c], A. Venturi[a], P.G. Verdini[a]

INFN Sezione di Roma[a], Sapienza Università di Roma[b], Roma, Italy
P. Akrap[a,b], C. Basile[a,b], S.C. Behera[a], F. Cavallari[a], L. Cunqueiro Mendez[a,b], F. De Riggi[a,b], D. Del Re[a,b], M. Del Vecchio[a,b], E. Di Marco[a], M. Diemoz[a], F. Errico[a], L. Frosina[a,b], R. Gargiulo[a,b], B. Harikrishnan[a,b], F. Lombardi[a,b], E. Longo[a,b], L. Martikainen[a,b], J. Mijuskovic[a,b], G. Organtini[a,b], N. Palmeri[a,b], R. Paramatti[a,b], T. Pauletto[a,b], S. Rahatlou[a,b], C. Rovelli[a], F. Santanastasio[a,b], L. Soffi[a], V. Vladimirov[a,b]

INFN Sezione di Torino[a], Università di Torino[b], Torino, Italy; Università del Piemonte Orientale[c], Novara, Italy
N. Amapane[a,b], R. Arcidiacono[a,c], S. Argiro[a,b], M. Arneodo[†a,c], N. Bartosik[a,c], R. Bellan[a,b], A. Bellora[a,b], C. Biino[a], C. Borca[a,b], N. Cartiglia[a], M. Costa[a,b], R. Covarelli[a,b], N. Demaria[a], L. Finco[a], M. Grippo[a,b], B. Kiani[a,b], L. Lanteri[a,b], F. Legger[a], F. Luongo[a,b], C. Mariotti[a], S. Maselli[a], A. Mecca[a,b], L. Menzio[a,b], P. Meridiani[a], E. Migliore[a,b], M. Monteno[a], M.M. Obertino[a,b], G. Ortona[a], L. Pacher[a,b], N. Pastrone[a], M. Ruspa[a,c], F. Siviero[a,b], V. Sola[a,b], A. Solano[a,b], A. Staiano[a], C. Tarricone[a,b], D. Trocino[a], G. Umoret[a,b], E. Vlasov[a,b], R. White[a,b]

INFN Sezione di Trieste[a], Università di Trieste[b], Trieste, Italy
J. Babbar[a,b,52], S. Belforte[a], V. Candelise[a,b], M. Casarsa[a], F. Cossutti[a], K. De Leo[a], G. Della Ricca[a,b], R. Delli Gatti[a,b]

Kyungpook National University, Daegu, Korea
S. Dogra, J. Hong, J. Kim, T. Kim, D. Lee, H. Lee, J. Lee, S.W. Lee, C.S. Moon, Y.D. Oh, S. Sekmen, B. Tae, Y.C. Yang

Department of Mathematics and Physics - GWNU, Gangneung, Korea
M.S. Kim

Chonnam National University, Institute for Universe and Elementary Particles, Kwangju, Korea
G. Bak, P. Gwak, H. Kim, D.H. Moon, J. Seo

Hanyang University, Seoul, Korea
E. Asilar, F. Carnevali, J. Choi[53], T.J. Kim, Y. Ryou, J. Song

Korea University, Seoul, Korea
S. Ha, S. Han, B. Hong, J. Kim, K. Lee, K.S. Lee, S. Lee, J. Yoo

Kyung Hee University, Department of Physics, Seoul, Korea
J. Goh, J. Shin, S. Yang

Sejong University, Seoul, Korea
Y. Kang, H. S. Kim, Y. Kim, B. Ko, S. Lee

Seoul National University, Seoul, Korea

J. Almond, J.H. Bhyun, J. Choi, J. Choi, W. Jun, H. Kim, J. Kim, T. Kim, Y. Kim, Y.W. Kim, S. Ko, H. Lee, J. Lee, J. Lee, B.H. Oh, J. Shin, U.K. Yang, I. Yoon

University of Seoul, Seoul, Korea
W. Jang, D. Kim, S. Kim, J.S.H. Lee, Y. Lee, I.C. Park, Y. Roh, I.J. Watson

Yonsei University, Department of Physics, Seoul, Korea
G. Cho, K. Hwang, B. Kim, S. Kim, K. Lee, H.D. Yoo

Sungkyunkwan University, Suwon, Korea
Y. Lee, I. Yu

College of Engineering and Technology, American University of the Middle East (AUM), Dasman, Kuwait
T. Beyrouthy, Y. Gharbia

Kuwait University - College of Science - Department of Physics, Safat, Kuwait
F. Alazemi

Riga Technical University, Riga, Latvia
K. Dreimanis, O.M. Eberlins, A. Gaile, C. Munoz Diaz, D. Osite, G. Pikurs, R. Plese, A. Potrebko, M. Seidel, D. Sidiropoulos Kontos

University of Latvia (LU), Riga, Latvia
N.R. Strautnieks

Vilnius University, Vilnius, Lithuania
M. Ambrozas, A. Juodagalvis, S. Nargelas, A. Rinkevicius, G. Tamulaitis

National Centre for Particle Physics, Universiti Malaya, Kuala Lumpur, Malaysia
I. Yusuff[54], Z. Zolkapli

Universidad de Sonora (UNISON), Hermosillo, Mexico
J.F. Benitez, A. Castaneda Hernandez, A. Cota Rodriguez, L.E. Cuevas Picos, H.A. Encinas Acosta, L.G. Gallegos Maríñez, J.A. Murillo Quijada, L. Valencia Palomo

Centro de Investigacion y de Estudios Avanzados del IPN, Mexico City, Mexico
G. Ayala, H. Castilla-Valdez, H. Crotte Ledesma, R. Lopez-Fernandez, J. Mejia Guisao, R. Reyes-Almanza, A. Sánchez Hernández

Universidad Iberoamericana, Mexico City, Mexico
C. Oropeza Barrera, D.L. Ramirez Guadarrama, M. Ramírez García

Benemerita Universidad Autonoma de Puebla, Puebla, Mexico
I. Bautista, F.E. Neri Huerta, I. Pedraza, H.A. Salazar Ibarguen, C. Uribe Estrada

University of Montenegro, Podgorica, Montenegro
I. Bubanja, N. Raicevic

University of Canterbury, Christchurch, New Zealand
P.H. Butler

National Centre for Physics, Quaid-I-Azam University, Islamabad, Pakistan
A. Ahmad, M.I. Asghar, A. Awais, M.I.M. Awan, W.A. Khan

AGH University of Krakow, Krakow, Poland
V. Avati, L. Forthomme, L. Grzanka, M. Malawski, K. Piotrzkowski

National Centre for Nuclear Research, Swierk, Poland
M. Bluj, M. Górski, M. Kazana, M. Szleper, P. Zalewski

Institute of Experimental Physics, Faculty of Physics, University of Warsaw, Warsaw, Poland
K. Bunkowski, K. Doroba, A. Kalinowski, M. Konecki, J. Krolikowski, A. Muhammad

Warsaw University of Technology, Warsaw, Poland
P. Fokow, K. Pozniak, W. Zabolotny

Laboratório de Instrumentação e Física Experimental de Partículas, Lisboa, Portugal
M. Araujo, D. Bastos, C. Beirão Da Cruz E Silva, A. Boletti, M. Bozzo, T. Camporesi, G. Da Molin, M. Gallinaro, J. Hollar, N. Leonardo, G.B. Marozzo, A. Petrilli, M. Pisano, J. Seixas, J. Varela, J.W. Wulff

Faculty of Physics, University of Belgrade, Belgrade, Serbia
P. Adzic, L. Markovic, P. Milenovic, V. Milosevic

VINCA Institute of Nuclear Sciences, University of Belgrade, Belgrade, Serbia
D. Devetak, M. Dordevic, J. Milosevic, L. Nadderd, V. Rekovic, M. Stojanovic

Centro de Investigaciones Energéticas Medioambientales y Tecnológicas (CIEMAT), Madrid, Spain
M. Alcalde Martinez, J. Alcaraz Maestre, Cristina F. Bedoya, J.A. Brochero Cifuentes, Oliver M. Carretero, M. Cepeda, M. Cerrada, N. Colino, B. De La Cruz, A. Delgado Peris, A. Escalante Del Valle, D. Fernández Del Val, J.P. Fernández Ramos, J. Flix, M.C. Fouz, M. Gonzalez Hernandez, O. Gonzalez Lopez, S. Goy Lopez, J.M. Hernandez, M.I. Josa, J. Llorente Merino, C. Martin Perez, E. Martin Viscasillas, D. Moran, C. M. Morcillo Perez, Á. Navarro Tobar, R. Paz Herrera, A. Pérez-Calero Yzquierdo, J. Puerta Pelayo, I. Redondo, J. Vazquez Escobar

Universidad Autónoma de Madrid, Madrid, Spain
J.F. de Trocóniz

Universidad de Oviedo, Instituto Universitario de Ciencias y Tecnologías Espaciales de Asturias (ICTEA), Oviedo, Spain
B. Alvarez Gonzalez, J. Ayllon Torresano, A. Cardini, J. Cuevas, J. Del Riego Badas, D. Estrada Acevedo, J. Fernandez Menendez, S. Folgueras, I. Gonzalez Caballero, P. Leguina, M. Obeso Menendez, E. Palencia Cortezon, J. Prado Pico, A. Soto Rodríguez, P. Vischia

Instituto de Física de Cantabria (IFCA), CSIC-Universidad de Cantabria, Santander, Spain
S. Blanco Fernández, I.J. Cabrillo, A. Calderon, J. Duarte Campderros, M. Fernandez, G. Gomez, C. Lasaosa García, R. Lopez Ruiz, C. Martinez Rivero, P. Martinez Ruiz del Arbol, F. Matorras, P. Matorras Cuevas, E. Navarrete Ramos, J. Piedra Gomez, C. Quintana San Emeterio, L. Scodellaro, I. Vila, R. Vilar Cortabitarte, J.M. Vizan Garcia

University of Colombo, Colombo, Sri Lanka
B. Kailasapathy[55], D.D.C. Wickramarathna

University of Ruhuna, Department of Physics, Matara, Sri Lanka
W.G.D. Dharmaratna[56], K. Liyanage, N. Perera

CERN, European Organization for Nuclear Research, Geneva, Switzerland

D. Abbaneo, C. Amendola, R. Ardino, E. Auffray, J. Baechler, D. Barney, J. Bendavid, M. Bianco, A. Bocci, L. Borgonovi, C. Botta, A. Bragagnolo, C.E. Brown, C. Caillol, G. Cerminara, P. Connor, K. Cormier, D. d'Enterria, A. Dabrowski, A. David, A. De Roeck, M.M. Defranchis, M. Deile, M. Dobson, P.J. Fernández Manteca, B.A. Fontana Santos Alves, E. Fontanesi, W. Funk, A. Gaddi, S. Giani, D. Gigi, K. Gill, F. Glege, M. Glowacki, A. Gruber, J. Hegeman, J.K. Heikkilä, R. Hofsaess, B. Huber, T. James, P. Janot, O. Kaluzinska, O. Karacheban[25], G. Karathanasis, S. Laurila, P. Lecoq, E. Leutgeb, C. Lourenço, A.-M. Lyon, M. Magherini, L. Malgeri, M. Mannelli, A. Mehta, F. Meijers, J.A. Merlin, S. Mersi, E. Meschi, M. Migliorini, F. Monti, F. Moortgat, M. Mulders, M. Musich, I. Neutelings, S. Orfanelli, F. Pantaleo, M. Pari, G. Petrucciani, A. Pfeiffer, M. Pierini, M. Pitt, H. Qu, D. Rabady, A. Reimers, B. Ribeiro Lopes, F. Riti, P. Rosado, M. Rovere, H. Sakulin, R. Salvatico, S. Sanchez Cruz, S. Scarfi, M. Selvaggi, K. Shchelina, P. Silva, P. Sphicas[57], A.G. Stahl Leiton, A. Steen, S. Summers, D. Treille, P. Tropea, E. Vernazza, J. Wanczyk[58], S. Wuchterl, M. Zarucki, P. Zehetner, P. Zejdl, G. Zevi Della Porta

PSI Center for Neutron and Muon Sciences, Villigen, Switzerland
L. Caminada[59], W. Erdmann, R. Horisberger, Q. Ingram, H.C. Kaestli, D. Kotlinski, C. Lange, U. Langenegger, A. Nigamova, L. Noehte[59], T. Rohe, A. Samalan

ETH Zurich - Institute for Particle Physics and Astrophysics (IPA), Zurich, Switzerland
T.K. Aarrestad, M. Backhaus, T. Bevilacqua[59], G. Bonomelli, C. Cazzaniga, K. Datta, P. De Bryas Dexmiers D'Archiacchiac[58], A. De Cosa, G. Dissertori, M. Dittmar, M. Donegà, F. Glessgen, C. Grab, N. Härringer, T.G. Harte, W. Lustermann, M. Malucchi, R.A. Manzoni, L. Marchese, A. Mascellani[58], F. Nessi-Tedaldi, F. Pauss, B. Ristic, R. Seidita, J. Steggemann[58], A. Tarabini, D. Valsecchi, R. Wallny

Universität Zürich, Zurich, Switzerland
C. Amsler[60], P. Bärtschi, F. Bilandzija, M.F. Canelli, G. Celotto, V. Guglielmi, A. Jofrehei, B. Kilminster, T.H. Kwok, S. Leontsinis, V. Lukashenko, A. Macchiolo, F. Meng, M. Missiroli, J. Motta, P. Robmann, E. Shokr, F. Stäger, R. Tramontano, P. Viscone

National Central University, Chung-Li, Taiwan
D. Bhowmik, C.M. Kuo, P.K. Rout, S. Taj, P.C. Tiwari[36]

National Taiwan University (NTU), Taipei, Taiwan
L. Ceard, K.F. Chen, Z.g. Chen, A. De Iorio, W.-S. Hou, T.h. Hsu, Y.w. Kao, S. Karmakar, G. Kole, Y.y. Li, R.-S. Lu, E. Paganis, X.f. Su, J. Thomas-Wilsker, L.s. Tsai, D. Tsionou, H.y. Wu, E. Yazgan

High Energy Physics Research Unit, Department of Physics, Faculty of Science, Chulalongkorn University, Bangkok, Thailand
C. Asawatangtrakuldee, N. Srimanobhas

Tunis El Manar University, Tunis, Tunisia
Y. Maghrbi

Çukurova University, Physics Department, Science and Art Faculty, Adana, Turkey
D. Agyel, F. Dolek, I. Dumanoglu[61], Y. Guler[62], E. Gurpinar Guler[62], C. Isik,

O. Kara[63], A. Kayis Topaksu, Y. Komurcu, G. Onengut, K. Ozdemir[64], B. Tali[65], U.G. Tok, E. Uslan, I.S. Zorbakir

Hacettepe University, Ankara, Turkey
S. Sen

Middle East Technical University, Physics Department, Ankara, Turkey
M. Yalvac[66]

Bogazici University, Istanbul, Turkey
B. Akgun, I.O. Atakisi[67], E. Gülmez, M. Kaya[68], O. Kaya[69], M.A. Sarkisla[70], S. Tekten[71]

Istanbul Technical University, Istanbul, Turkey
D. Boncukcu, A. Cakir, K. Cankocak[61,72]

Istanbul University, Istanbul, Turkey
B. Hacisahinoglu, I. Hos[73], B. Kaynak, S. Ozkorucuklu, O. Potok, H. Sert, C. Simsek, C. Zorbilmez

Yildiz Technical University, Istanbul, Turkey
S. Cerci, C. Dozen[74], B. Isildak, E. Simsek, D. Sunar Cerci, T. Yetkin[74]

Institute for Scintillation Materials of National Academy of Science of Ukraine, Kharkiv, Ukraine
A. Boyaryntsev, O. Dadazhanova, B. Grynyov

National Science Centre, Kharkiv Institute of Physics and Technology, Kharkiv, Ukraine
L. Levchuk

University of Bristol, Bristol, United Kingdom
J.J. Brooke, A. Bundock, F. Bury, E. Clement, D. Cussans, D. Dharmender, H. Flacher, J. Goldstein, H.F. Heath, M.-L. Holmberg, L. Kreczko, S. Paramesvaran, L. Robertshaw, M.S. Sanjrani[39], J. Segal, V.J. Smith

Rutherford Appleton Laboratory, Didcot, United Kingdom
A.H. Ball, K.W. Bell, A. Belyaev[75], C. Brew, R.M. Brown, D.J.A. Cockerill, A. Elliot, K.V. Ellis, J. Gajownik, K. Harder, S. Harper, J. Linacre, K. Manolopoulos, M. Moallemi, D.M. Newbold, E. Olaiya, D. Petyt, T. Reis, A.R. Sahasransu, G. Salvi, T. Schuh, C.H. Shepherd-Themistocleous, I.R. Tomalin, K.C. Whalen, T. Williams

Imperial College, London, United Kingdom
I. Andreou, R. Bainbridge, P. Bloch, O. Buchmuller, C.A. Carrillo Montoya, D. Colling, I. Das, P. Dauncey, G. Davies, M. Della Negra, S. Fayer, G. Fedi, G. Hall, H.R. Hoorani, A. Howard, G. Iles, C.R. Knight, P. Krueper, J. Langford, K.H. Law, J. León Holgado, L. Lyons, A.-M. Magnan, B. Maier, S. Mallios, A. Mastronikolis, M. Mieskolainen, J. Nash[76], M. Pesaresi, P.B. Pradeep, B.C. Radburn-Smith, A. Richards, A. Rose, L. Russell, K. Savva, C. Seez, R. Shukla, A. Tapper, K. Uchida, G.P. Uttley, T. Virdee[27], M. Vojinovic, N. Wardle, D. Winterbottom

Brunel University, Uxbridge, United Kingdom
J.E. Cole, A. Khan, P. Kyberd, I.D. Reid

Baylor University, Waco, Texas, USA

S. Abdullin, A. Brinkerhoff, E. Collins, M.R. Darwish, J. Dittmann, K. Hatakeyama, V. Hegde, J. Hiltbrand, B. McMaster, J. Samudio, S. Sawant, C. Sutantawibul, J. Wilson

Bethel University, St. Paul, Minnesota, USA
J.M. Hogan

Catholic University of America, Washington, DC, USA
R. Bartek, A. Dominguez, S. Raj, B. Sahu, A.E. Simsek, S.S. Yu

The University of Alabama, Tuscaloosa, Alabama, USA
B. Bam, A. Buchot Perraguin, S. Campbell, R. Chudasama, S.I. Cooper, C. Crovella, G. Fidalgo, S.V. Gleyzer, A. Khukhunaishvili, K. Matchev, E. Pearson, P. Rumerio[77], E. Usai, R. Yi

Boston University, Boston, Massachusetts, USA
S. Cholak, G. De Castro, Z. Demiragli, C. Erice, C. Fangmeier, C. Fernandez Madrazo, J. Fulcher, F. Golf, S. Jeon, J. O'Cain, I. Reed, J. Rohlf, K. Salyer, D. Sperka, D. Spitzbart, I. Suarez, A. Tsatsos, E. Wurtz, A.G. Zecchinelli

Brown University, Providence, Rhode Island, USA
G. Barone, G. Benelli, D. Cutts, S. Ellis, L. Gouskos, M. Hadley, U. Heintz, K.W. Ho, T. Kwon, L. Lambrecht, G. Landsberg, K.T. Lau, J. Luo, S. Mondal, J. Roloff, T. Russell, S. Sagir[78], X. Shen, M. Stamenkovic, N. Venkatasubramanian

University of California, Davis, Davis, California, USA
S. Abbott, S. Baradia, B. Barton, R. Breedon, H. Cai, M. Calderon De La Barca Sanchez, E. Cannaert, M. Chertok, M. Citron, J. Conway, P.T. Cox, F. Eble, R. Erbacher, O. Kukral, G. Mocellin, S. Ostrom, I. Salazar Segovia, J.S. Tafoya Vargas, W. Wei, S. Yoo

University of California, Los Angeles, California, USA
K. Adamidis, M. Bachtis, D. Campos, R. Cousins, S. Crossley, G. Flores Avila, J. Hauser, M. Ignatenko, M.A. Iqbal, T. Lam, Y.f. Lo, E. Manca, A. Nunez Del Prado, D. Saltzberg, V. Valuev

University of California, Riverside, Riverside, California, USA
R. Clare, J.W. Gary, G. Hanson

University of California, San Diego, La Jolla, California, USA
A. Aportela, A. Arora, J.G. Branson, S. Cittolin, S. Cooperstein, B. D'Anzi, D. Diaz, J. Duarte, L. Giannini, Y. Gu, J. Guiang, V. Krutelyov, R. Lee, J. Letts, H. Li, M. Masciovecchio, F. Mokhtar, S. Mukherjee, M. Pieri, D. Primosch, M. Quinnan, V. Sharma, M. Tadel, E. Vourliotis, F. Würthwein, A. Yagil, Z. Zhao

University of California, Santa Barbara - Department of Physics, Santa Barbara, California, USA
A. Barzdukas, L. Brennan, C. Campagnari, S. Carron Montero[79], K. Downham, C. Grieco, M.M. Hussain, J. Incandela, M.W.K. Lai, A.J. Li, P. Masterson, J. Richman, S.N. Santpur, R. Schmitz, D. Stuart, T.Á. Vámi, X. Yan, D. Zhang

California Institute of Technology, Pasadena, California, USA
A. Albert, S. Bhattacharya, A. Bornheim, O. Cerri, R. Kansal, H.B. Newman, G. Reales Gutiérrez, T. Sievert, M. Spiropulu, J.R. Vlimant, R.A. Wynne, S. Xie

Carnegie Mellon University, Pittsburgh, Pennsylvania, USA
J. Alison, S. An, M. Cremonesi, V. Dutta, E.Y. Ertorer, T. Ferguson, T.A. Gómez Espinosa, A. Harilal, A. Kallil Tharayil, M. Kanemura, C. Liu, M. Marchegiani, P. Meiring, S. Murthy, P. Palit, K. Park, M. Paulini, A. Roberts, A. Sanchez, W. Terrill

University of Colorado Boulder, Boulder, Colorado, USA
J.P. Cumalat, W.T. Ford, A. Hart, S. Kwan, J. Pearkes, C. Savard, N. Schonbeck, K. Stenson, K.A. Ulmer, S.R. Wagner, N. Zipper, D. Zuolo

Cornell University, Ithaca, New York, USA
J. Alexander, X. Chen, J. Dickinson, A. Duquette, J. Fan, X. Fan, J. Grassi, S. Hogan, P. Kotamnives, J. Monroy, G. Niendorf, M. Oshiro, J.R. Patterson, A. Ryd, J. Thom, P. Wittich, R. Zou, L. Zygala

Fermi National Accelerator Laboratory, Batavia, Illinois, USA
M. Albrow, M. Alyari, O. Amram, G. Apollinari, A. Apresyan, L.A.T. Bauerdick, D. Berry, J. Berryhill, P.C. Bhat, K. Burkett, J.N. Butler, A. Canepa, G.B. Cerati, H.W.K. Cheung, F. Chlebana, C. Cosby, G. Cummings, I. Dutta, V.D. Elvira, J. Freeman, A. Gandrakota, Z. Gecse, L. Gray, D. Green, A. Grummer, S. Grünendahl, D. Guerrero, O. Gutsche, R.M. Harris, J. Hirschauer, V. Innocente, B. Jayatilaka, S. Jindariani, M. Johnson, U. Joshi, B. Klima, S. Lammel, C. Lee, D. Lincoln, R. Lipton, T. Liu, K. Maeshima, D. Mason, P. McBride, P. Merkel, S. Mrenna, S. Nahn, J. Ngadiuba, D. Noonan, S. Norberg, V. Papadimitriou, N. Pastika, K. Pedro, C. Pena[80], C.E. Perez Lara, V. Perovic, F. Ravera, A. Reinsvold Hall[81], L. Ristori, M. Safdari, E. Sexton-Kennedy, E. Smith, N. Smith, A. Soha, L. Spiegel, S. Stoynev, J. Strait, L. Taylor, S. Tkaczyk, N.V. Tran, L. Uplegger, E.W. Vaandering, C. Wang, I. Zoi

University of Florida, Gainesville, Florida, USA
C. Aruta, P. Avery, D. Bourilkov, P. Chang, V. Cherepanov, R.D. Field, C. Huh, E. Koenig, M. Kolosova, J. Konigsberg, A. Korytov, G. Mitselmakher, K. Mohrman, A. Muthirakalayil Madhu, N. Rawal, S. Rosenzweig, V. Sulimov, Y. Takahashi, J. Wang

Florida State University, Tallahassee, Florida, USA
T. Adams, A. Al Kadhim, A. Askew, S. Bower, R. Goff, R. Hashmi, A. Hassani, R.S. Kim, T. Kolberg, G. Martinez, M. Mazza, H. Prosper, P.R. Prova, R. Yohay

Florida Institute of Technology, Melbourne, Florida, USA
B. Alsufyani, S. Butalla, S. Das, M. Hohlmann, M. Lavinsky, E. Yanes

University of Illinois Chicago, Chicago, Illinois, USA
M.R. Adams, N. Barnett, A. Baty, C. Bennett, R. Cavanaugh, R. Escobar Franco, O. Evdokimov, C.E. Gerber, H. Gupta, M. Hawksworth, A. Hingrajiya, D.J. Hofman, Z. Huang, J.h. Lee, C. Mills, S. Nanda, G. Nigmatkulov, B. Ozek, T. Phan, D. Pilipovic, R. Pradhan, E. Prifti, P. Roy, T. Roy, D. Shekar, N. Singh, A. Thielen, M.B. Tonjes, N. Varelas, M.A. Wadud, J. Yoo

The University of Iowa, Iowa City, Iowa, USA
M. Alhusseini, D. Blend, K. Dilsiz[82], O.K. Köseyan, A. Mestvirishvili[83], O. Neogi, H. Ogul[84], Y. Onel, A. Penzo, C. Snyder, E. Tiras[85]

Johns Hopkins University, Baltimore, Maryland, USA

B. Blumenfeld, J. Davis, A.V. Gritsan, L. Kang, S. Kyriacou, P. Maksimovic, M. Roguljic, S. Sekhar, M.V. Srivastav, M. Swartz

The University of Kansas, Lawrence, Kansas, USA
A. Abreu, L.F. Alcerro Alcerro, J. Anguiano, S. Arteaga Escatel, P. Baringer, A. Bean, R. Bhattacharya, Z. Flowers, D. Grove, J. King, G. Krintiras, M. Lazarovits, C. Le Mahieu, J. Marquez, M. Murray, M. Nickel, S. Popescu[86], C. Rogan, C. Royon, S. Rudrabhatla, S. Sanders, C. Smith, G. Wilson

Kansas State University, Manhattan, Kansas, USA
B. Allmond, N. Islam, A. Ivanov, K. Kaadze, Y. Maravin, J. Natoli, G.G. Reddy, D. Roy, G. Sorrentino

University of Maryland, College Park, Maryland, USA
A. Baden, A. Belloni, J. Bistany-riebman, S.C. Eno, N.J. Hadley, S. Jabeen, R.G. Kellogg, T. Koeth, B. Kronheim, S. Lascio, P. Major, A.C. Mignerey, C. Palmer, C. Papageorgakis, M.M. Paranjpe, E. Popova[87], A. Shevelev, L. Zhang

Massachusetts Institute of Technology, Cambridge, Massachusetts, USA
C. Baldenegro Barrera, H. Bossi, S. Bright-Thonney, I.A. Cali, Y.c. Chen, P.c. Chou, M. D'Alfonso, J. Eysermans, C. Freer, G. Gomez-Ceballos, M. Goncharov, G. Grosso, P. Harris, D. Hoang, G.M. Innocenti, K. Ivanov, G. Kopp, D. Kovalskyi, J. Krupa, L. Lavezzo, Y.-J. Lee, K. Long, C. Mcginn, A. Novak, M.I. Park, C. Paus, C. Reissel, C. Roland, G. Roland, S. Rothman, T.a. Sheng, G.S.F. Stephans, D. Walter, J. Wang, Z. Wang, B. Wyslouch, T. J. Yang

University of Minnesota, Minneapolis, Minnesota, USA
A. Alpana, B. Crossman, W.J. Jackson, C. Kapsiak, M. Krohn, D. Mahon, J. Mans, B. Marzocchi, R. Rusack, O. Sancar, R. Saradhy, N. Strobbe

University of Nebraska-Lincoln, Lincoln, Nebraska, USA
K. Bloom, D.R. Claes, G. Haza, J. Hossain, C. Joo, I. Kravchenko, K.H.M. Kwok, A. Rohilla, J.E. Siado, W. Tabb, A. Vagnerini, A. Wightman, F. Yan

State University of New York at Buffalo, Buffalo, New York, USA
H. Bandyopadhyay, L. Hay, H.w. Hsia, I. Iashvili, A. Kalogeropoulos, A. Kharchilava, A. Mandal, M. Morris, D. Nguyen, S. Rappoccio, H. Rejeb Sfar, A. Williams, D. Yu

Northeastern University, Boston, Massachusetts, USA
A. Aarif, G. Alverson, E. Barberis, J. Bonilla, B. Bylsma, M. Campana, J. Dervan, Y. Haddad, Y. Han, I. Israr, A. Krishna, M. Lu, N. Manganelli, R. Mccarthy, D.M. Morse, T. Orimoto, L. Skinnari, C.S. Thoreson, E. Tsai, D. Wood

Northwestern University, Evanston, Illinois, USA
S. Dittmer, K.A. Hahn, M. Mcginnis, Y. Miao, D.G. Monk, M.H. Schmitt, A. Taliercio, M. Velasco, J. Wang

University of Notre Dame, Notre Dame, Indiana, USA
G. Agarwal, R. Band, R. Bucci, S. Castells, A. Das, A. Datta, A. Ehnis, R. Goldouzian, M. Hildreth, K. Hurtado Anampa, T. Ivanov, C. Jessop, A. Karneyeu, K. Lannon, J. Lawrence, N. Loukas, L. Lutton, J. Mariano, N. Marinelli, T. McCauley, C. Mcgrady, C. Moore, Y. Musienko[21], H. Nelson,

M. Osherson, A. Piccinelli, R. Ruchti, A. Townsend, Y. Wan, M. Wayne, H. Yockey

The Ohio State University, Columbus, Ohio, USA
M. Carrigan, R. De Los Santos, L.S. Durkin, C. Hill, M. Joyce, D.A. Wenzl, B.L. Winer, B. R. Yates

Princeton University, Princeton, New Jersey, USA
H. Bouchamaoui, G. Dezoort, P. Elmer, A. Frankenthal, M. Galli, B. Greenberg, N. Haubrich, K. Kennedy, Y. Lai, D. Lange, A. Loeliger, D. Marlow, I. Ojalvo, J. Olsen, F. Simpson, D. Stickland, C. Tully

University of Puerto Rico, Mayaguez, Puerto Rico, USA
S. Malik, R. Sharma

Purdue University, West Lafayette, Indiana, USA
S. Chandra, A. Gu, L. Gutay, M. Huwiler, M. Jones, A.W. Jung, D. Kondratyev, J. Li, M. Liu, G. Negro, N. Neumeister, G. Paspalaki, S. Piperov, N.R. Saha, J.F. Schulte, F. Wang, A. Wildridge, W. Xie, Y. Yao, Y. Zhong

Purdue University Northwest, Hammond, Indiana, USA
N. Parashar, A. Pathak, E. Shumka

Rice University, Houston, Texas, USA
D. Acosta, A. Agrawal, C. Arbour, T. Carnahan, P. Das, K.M. Ecklund, F.J.M. Geurts, T. Huang, I. Krommydas, N. Lewis, W. Li, J. Lin, O. Miguel Colin, B.P. Padley, R. Redjimi, J. Rotter, C. Vico Villalba, M. Wulansatiti, E. Yigitbasi, Y. Zhang

University of Rochester, Rochester, New York, USA
O. Bessidskaia Bylund, A. Bodek, P. de Barbaro[†], R. Demina, A. Garcia-Bellido, H.S. Hare, O. Hindrichs, N. Parmar, P. Parygin[87], H. Seo, R. Taus

Rutgers, The State University of New Jersey, Piscataway, New Jersey, USA
B. Chiarito, J.P. Chou, S.V. Clark, S. Donnelly, D. Gadkari, Y. Gershtein, E. Halkiadakis, C. Houghton, D. Jaroslawski, A. Kobert, I. Laflotte, A. Lath, J. Martins, M. Perez Prada, B. Rand, J. Reichert, P. Saha, S. Salur, S. Somalwar, R. Stone, S.A. Thayil, S. Thomas, J. Vora

University of Tennessee, Knoxville, Tennessee, USA
D. Ally, A.G. Delannoy, S. Fiorendi, J. Harris, T. Holmes, A.R. Kanuganti, N. Karunarathna, J. Lawless, L. Lee, E. Nibigira, B. Skipworth, S. Spanier

Texas A&M University, College Station, Texas, USA
D. Aebi, M. Ahmad, T. Akhter, K. Androsov, A. Basnet, A. Bolshov, O. Bouhali[88], A. Cagnotta, V. D'Amante, R. Eusebi, P. Flanagan, J. Gilmore, Y. Guo, T. Kamon, S. Luo, R. Mueller, A. Safonov

Texas Tech University, Lubbock, Texas, USA
N. Akchurin, J. Damgov, Y. Feng, N. Gogate, W. Jin, S.W. Lee, C. Madrid, A. Mankel, T. Peltola, I. Volobouev

Vanderbilt University, Nashville, Tennessee, USA
E. Appelt, Y. Chen, S. Greene, A. Gurrola, W. Johns, R. Kunnawalkam Elayavalli, A. Melo, D. Rathjens, F. Romeo, P. Sheldon, S. Tuo, J. Velkovska, J. Viinikainen, J. Zhang

University of Virginia, Charlottesville, Virginia, USA
B. Cardwell, H. Chung, B. Cox, J. Hakala, G. Hamilton Ilha Machado, R. Hirosky, M. Jose, A. Ledovskoy, C. Mantilla, C. Neu, C. Ramón Álvarez, Z. Wu

Wayne State University, Detroit, Michigan, USA
S. Bhattacharya, P.E. Karchin

University of Wisconsin - Madison, Madison, Wisconsin, USA
A. Aravind, S. Banerjee, K. Black, T. Bose, E. Chavez, S. Dasu, P. Everaerts, C. Galloni, H. He, M. Herndon, A. Herve, C.K. Koraka, S. Lomte, R. Loveless, A. Mallampalli, A. Mohammadi, S. Mondal, T. Nelson, G. Parida, L. Pétré, D. Pinna, A. Savin, V. Shang, V. Sharma, W.H. Smith, D. Teague, A. Warden

Authors affiliated with an international laboratory covered by a cooperation agreement with CERN
S. Afanasiev, V. Alexakhin, Yu. Andreev, T. Aushev, D. Budkouski, R. Chistov, M. Danilov, T. Dimova, A. Ershov, S. Gninenko, I. Gorbunov, A. Gribushin, A. Kamenev, V. Karjavine, M. Kirsanov, V. Klyukhin, O. Kodolova[89], V. Korenkov, I. Korsakov, A. Kozyrev, N. Krasnikov, A. Lanev, A. Malakhov, V. Matveev, A. Nikitenko[90,89], V. Palichik, V. Perelygin, S. Petrushanko, O. Radchenko, M. Savina, V. Shalaev, S. Shmatov, S. Shulha, Y. Skovpen, K. Slizhevskiy, V. Smirnov, O. Teryaev, I. Tlisova, A. Toropin, N. Voytishin, A. Zarubin, I. Zhizhin

Authors affiliated with an institute formerly covered by a cooperation agreement with CERN
E. Boos, V. Bunichev, M. Dubinin[80], V. Savrin, A. Snigirev, L. Dudko, V. Kim[21], V. Murzin, V. Oreshkin, D. Sosnov

†: Deceased
[1]Also at Yerevan State University, Yerevan, Armenia
[2]Also at TU Wien, Vienna, Austria
[3]Also at Ghent University, Ghent, Belgium
[4]Also at FACAMP - Faculdades de Campinas, Sao Paulo, Brazil
[5]Also at Universidade Estadual de Campinas, Campinas, Brazil
[6]Also at Federal University of Rio Grande do Sul, Porto Alegre, Brazil
[7]Also at The University of the State of Amazonas, Manaus, Brazil
[8]Also at University of Chinese Academy of Sciences, Beijing, China
[9]Also at University of Chinese Academy of Sciences, Beijing, China
[10]Also at School of Physics, Zhengzhou University, Zhengzhou, China
[11]Now at Henan Normal University, Xinxiang, China
[12]Also at University of Shanghai for Science and Technology, Shanghai, China
[13]Also at The University of Iowa, Iowa City, Iowa, USA
[14]Also at Nanjing Normal University, Nanjing, China
[15]Also at Center for High Energy Physics, Peking University, Beijing, China
[16]Also at Cairo University, Cairo, Egypt
[17]Also at Suez University, Suez, Egypt
[18]Now at British University in Egypt, Cairo, Egypt
[19]Also at Purdue University, West Lafayette, Indiana, USA
[20]Also at Université de Haute Alsace, Mulhouse, France
[21]Also at an institute formerly covered by a cooperation agreement with CERN
[22]Also at University of Hamburg, Hamburg, Germany
[23]Also at RWTH Aachen University, III. Physikalisches Institut A, Aachen, Germany

[24]Also at Bergische University Wuppertal (BUW), Wuppertal, Germany
[25]Also at Brandenburg University of Technology, Cottbus, Germany
[26]Also at Forschungszentrum Jülich, Juelich, Germany
[27]Also at CERN, European Organization for Nuclear Research, Geneva, Switzerland
[28]Also at HUN-REN ATOMKI - Institute of Nuclear Research, Debrecen, Hungary
[29]Now at Universitatea Babes-Bolyai - Facultatea de Fizica, Cluj-Napoca, Romania
[30]Also at MTA-ELTE Lendület CMS Particle and Nuclear Physics Group, Eötvös Loránd University, Budapest, Hungary
[31]Also at HUN-REN Wigner Research Centre for Physics, Budapest, Hungary
[32]Also at Physics Department, Faculty of Science, Assiut University, Assiut, Egypt
[33]Also at The University of Kansas, Lawrence, Kansas, USA
[34]Also at Punjab Agricultural University, Ludhiana, India
[35]Also at University of Hyderabad, Hyderabad, India
[36]Also at Indian Institute of Science (IISc), Bangalore, India
[37]Also at University of Visva-Bharati, Santiniketan, India
[38]Also at Institute of Physics, Bhubaneswar, India
[39]Also at Deutsches Elektronen-Synchrotron, Hamburg, Germany
[40]Also at Isfahan University of Technology, Isfahan, Iran
[41]Also at Sharif University of Technology, Tehran, Iran
[42]Also at Department of Physics, University of Science and Technology of Mazandaran, Behshahr, Iran
[43]Also at Department of Physics, Faculty of Science, Arak University, ARAK, Iran
[44]Also at Helwan University, Cairo, Egypt
[45]Also at Italian National Agency for New Technologies, Energy and Sustainable Economic Development, Bologna, Italy
[46]Also at Centro Siciliano di Fisica Nucleare e di Struttura Della Materia, Catania, Italy
[47]Also at Università degli Studi Guglielmo Marconi, Roma, Italy
[48]Also at Scuola Superiore Meridionale, Università di Napoli 'Federico II', Napoli, Italy
[49]Also at Fermi National Accelerator Laboratory, Batavia, Illinois, USA
[50]Also at Lulea University of Technology, Lulea, Sweden
[51]Also at Consiglio Nazionale delle Ricerche - Istituto Officina dei Materiali, Perugia, Italy
[52]Also at UPES - University of Petroleum and Energy Studies, Dehradun, India
[53]Also at Institut de Physique des 2 Infinis de Lyon (IP2I), Villeurbanne, France
[54]Also at Department of Applied Physics, Faculty of Science and Technology, Universiti Kebangsaan Malaysia, Bangi, Malaysia
[55]Also at Trincomalee Campus, Eastern University, Sri Lanka, Nilaveli, Sri Lanka
[56]Also at Saegis Campus, Nugegoda, Sri Lanka
[57]Also at National and Kapodistrian University of Athens, Athens, Greece
[58]Also at Ecole Polytechnique Fédérale Lausanne, Lausanne, Switzerland
[59]Also at Universität Zürich, Zurich, Switzerland
[60]Also at Stefan Meyer Institute for Subatomic Physics, Vienna, Austria
[61]Also at Near East University, Research Center of Experimental Health Science, Mersin, Turkey
[62]Also at Konya Technical University, Konya, Turkey
[63]Also at Istanbul Topkapi University, Istanbul, Turkey
[64]Also at Izmir Bakircay University, Izmir, Turkey
[65]Also at Adiyaman University, Adiyaman, Turkey
[66]Also at Bozok Universitetesi Rektörlügü, Yozgat, Turkey
[67]Also at Istanbul Sabahattin Zaim University, Istanbul, Turkey

[68]Also at Marmara University, Istanbul, Turkey
[69]Also at Milli Savunma University, Istanbul, Turkey
[70]Also at Informatics and Information Security Research Center, Gebze/Kocaeli, Turkey
[71]Also at Kafkas University, Kars, Turkey
[72]Now at Istanbul Okan University, Istanbul, Turkey
[73]Also at Istanbul University - Cerrahpasa, Faculty of Engineering, Istanbul, Turkey
[74]Also at Istinye University, Istanbul, Turkey
[75]Also at School of Physics and Astronomy, University of Southampton, Southampton, United Kingdom
[76]Also at Monash University, Faculty of Science, Clayton, Australia
[77]Also at Università di Torino, Torino, Italy
[78]Also at Karamanoğlu Mehmetbey University, Karaman, Turkey
[79]Also at California Lutheran University;, Thousand Oaks, California, USA
[80]Also at California Institute of Technology, Pasadena, California, USA
[81]Also at United States Naval Academy, Annapolis, Maryland, USA
[82]Also at Bingol University, Bingol, Turkey
[83]Also at Georgian Technical University, Tbilisi, Georgia
[84]Also at Sinop University, Sinop, Turkey
[85]Also at Erciyes University, Kayseri, Turkey
[86]Also at Horia Hulubei National Institute of Physics and Nuclear Engineering (IFIN-HH), Bucharest, Romania
[87]Now at another institute formerly covered by a cooperation agreement with CERN
[88]Also at Hamad Bin Khalifa University (HBKU), Doha, Qatar
[89]Also at Yerevan Physics Institute, Yerevan, Armenia
[90]Also at Imperial College, London, United Kingdom